https://doi.org/10.5194/egusphere-2026-2540
Preprint. Discussion started: 13 May 2026

Dynamic CO_2 evasion and colloidal control of trace metals in the Lower Lena River

Yuri Ya. Kolesnichenko[1], Sergey N. Vorobyev[1], Viktor A. Nikitkin[1], Oleg V. Dudarev[2], Denis V. Chernykh[2,3], Eduard A. Spivak[2,3], Arkadiy V. Kurilenko[2,3], Vladimir A. Kholodov[2], Igor P. Semiletov[2,3], Oleg S. Pokrovsky[4,5*]

[1]*National Research Tomsk State University (TSU), Lenina Ave., 36, Tomsk, 634050, Russia*
[2]*V.I. Il'ichev Pacific Oceanological Institute Far Eastern Branch Russian Academy of Science, Baltiyskaya st., 43, Vladivostok, 690041, Russia*
[3]*Sakhalin State University (SakhGU), Yuzhno Sakhalinsk , Russia*
[4]*Geosciences and Environment Toulouse, UMR 5563 CNRS, 14 Avenue Edouard Belin 31400 Toulouse, France*
[5]*N. Laverov Federal Center for Integrated Arctic Research, Russian Academy of Sciences, Arkhangelsk, Russia*

Key words: carbon, emission, permafrost, major elements, trace elements, Siberia

* email: oleg.pokrovski@cnrs.fr

https://doi.org/10.5194/egusphere-2026-2540
Preprint. Discussion started: 13 May 2026

Abstract

Large Arctic rivers integrate carbon and element fluxes across vast permafrost-dominated landscapes, yet the lower reaches of these systems remain poorly constrained in terms of greenhouse gas (GHG) emissions and solute organization. We investigated the Low Lena River over ~800 km during the beginning of summer baseflow, combining continuous in situ pCO_2 measurements, floating chamber flux determinations, and analyses of major and trace elements including colloidal size fractionation. CO_2 concentrations exhibited pronounced short-distance variability and weak northward decrease along the main stem. Diffusive CO_2 fluxes (0.1–1.3 g C m^{-2} d^{-1}) were comparable to values reported for other large Siberian rivers, confirming the Lena as a persistent but moderate atmospheric CO_2 source during the open-water season. In contrast, CH_4 concentrations were low and spatially uniform, contributing <0.5% to total carbon emissions. Notably, bulk DOC and DIC concentrations remained remarkably stable along the transect and were consistent with long-term monitoring records and previous expeditions, indicating strong buffering of dissolved carbon pools despite dynamic CO_2 evasion.

Major and trace elements segregated into two geochemical groups. Highly mobile major ions, Si, and selected oxyanion-forming trace elements were predominantly present in truly dissolved form (0–20% colloidal fraction) and reflected groundwater connectivity and water–rock interaction. In contrast, lithogenic low-solubility elements—including trivalent and tetravalent hydrolysates—were strongly associated with Fe–Al–organic colloids (>70%), indicating surface and suprapermafrost mobilization pathways. Multivariate statistics confirmed this dual organization of solute transport. These findings reveal a functional decoupling between structurally buffered dissolved carbon pools and dynamically regulated CO_2 exchange, a pattern likely characteristic of large Arctic rivers. Under ongoing warming, shifts in hydrological connectivity, discharge regime, and permafrost thaw may alter this balance, with implications for pan-Arctic carbon and element export to the Arctic Ocean.

https://doi.org/10.5194/egusphere-2026-2540
Preprint. Discussion started: 13 May 2026

Introduction

Greenhouse gas (GHG) emissions from inland waters in permafrost-affected regions constitute a critical component of the Arctic carbon cycle and represent one of the most important positive feedbacks to ongoing climate warming (Schuur et al., 2015). Permafrost thaw mobilizes large reservoirs of previously frozen organic carbon (OC), increasing its susceptibility to microbial degradation and atmospheric release, or promoting its lateral export to rivers and lakes (Frey and Smith, 2005; Vonk et al., 2019). Once transferred to aquatic systems, this carbon can be rapidly mineralized to CO_2 and CH_4 or transported downstream to the Arctic Ocean. In addition, macro- and micronutrients can be released from progressively thawing soils via surface flow or enhanced underground influx due to increasing connectivity with deep reservoirs therefore affecting coastal productivity and exerting biogeochemical control at the land – ocean interface (Frey et al., 2007; Tank et al., 2023).

For this reason, the biogeochemistry of dissolved organic carbon, major ions, and trace elements in Arctic rivers has been intensively investigated (Gordeev et al., 1996, 2004; Holmes et al., 2000, 2001; Tank et al., 2012; Drake et al., 2018; Kipp et al., 2020; Savenko and Savenko, 2024). Numerous studies have constrained seasonal export fluxes of dissolved and particulate constituents in major rivers (Holmes et al., 2012; Gordeev et al., 2024; Juhls et al., 2025), as well as in mid-sized systems and tributaries (Chupakov et al., 2020, 2023; Pokrovsky et al., 2010, 2022; Bagard et al., 2011; Krickov et al., 2025). These efforts have clarified how hydrological regime, permafrost thaw, and watershed characteristics regulate solute mobilization. However, much less attention has been paid to the spatial variability of CO_2 and CH_4 within river networks, and to their coupling with hydrochemistry and landscape structure during peak discharge. Furthermore, although this land–water–atmosphere continuum is widely recognized, in-situ data on GHG concentrations and emissions from major Siberian rivers—particularly during hydrologically dynamic periods—remain scarce.

Among the six great Arctic rivers, the Lena River is particularly emblematic. Draining nearly 2.5 million km² and flowing almost entirely within the continuous permafrost zone, it exhibits extreme seasonal discharge variability and documented increases in annual runoff (Yang et al., 2002; McClelland et al., 2004; Smith and Pavelsky, 2008; Ahmed et al., 2020). The basin encompasses extensive peatlands

https://doi.org/10.5194/egusphere-2026-2540
Preprint. Discussion started: 13 May 2026

and yedoma deposits rich in ancient OC that are increasingly affected by thaw (Zhang et al., 2005; Wild et al., 2019). These landscapes provide both modern and aged carbon to aquatic systems, potentially enhancing in-river GHG production during periods of intense lateral connectivity. While Lena River discharge (Berezovskaya et al., 2005; Ye et al., 2009; Tananaev et al., 2016; Gautier et al., 2018; Suzuki et al., 2018; Tananaev and Lotsari, 2022), sediment transport (Rachold et al., 1996; Dudarev et al., 2006), OC dynamics (Lara et al., 1998; Semiletov et al., 2011; Goncalvez-Araujo et al., 2015; Griffin et al., 2018; Ogneva et al., 2023), and hydrochemistry (Gordeev and Sidorov, 1993; Huh et al., 1998a,b; Georgiadi et al., 2019; Juhls et al., 2020) have been extensively documented, direct assessments of in-situ CO_2 and CH_4 concentrations and emissions along the main stem and its tributaries remain fragmentary. Existing GHG studies are largely confined to the Lena Delta (Kutzbach et al., 2007; Franz et al., 2016; Eckhardt et al., 2019; Beckebanze et al., 2022; Wegner et al., 2022) or upper reaches south of the Aldan River (Vorobyev et al., 2021a, b), leaving the ~800-km middle reach between Yakutsk and Kyusyur and several major tributaries (Vilyui, Muna, Molodo, Kyusyur) poorly constrained. This contrasts with more spatially integrated assessments conducted for the Yukon (Striegl et al., 2012), Mackenzie (Horan et al., 2019), and Ob (Pipko et al., 2019; Karlsson et al., 2021; Vorobyev et al., 2024).

Here, we present the first spatially integrated assessment of CO_2 and CH_4 concentrations and diffusive emissions along the Low Lena River main stem and key tributaries during the post-freshet recession period—a period of high hydrological connectivity and lateral carbon transfer. By coupling high-resolution hydrochemical measurements of major and trace solutes, in-situ CO_2 evasion, and colloidal assessment of trace element speciation in the main stem and tributaries, we evaluate spatial pattern of hydrological control on the main features of fluvial C and metal transport. We specifically test whether (i) tributaries draining peat- and yedoma-rich terrains act as disproportionate GHG hotspots relative to the main stem, and (ii) spatial patterns of CO_2 and CH_4 are systematically linked to DOC, major solutes, and trace-element signatures reflecting landscape controls. By resolving GHG dynamics across an 800-km river transect, this study provides the first spatially explicit evaluation of post-springtime carbon emissions from the lower Lena River system. Integrating gas fluxes with hydrochemistry and colloidal transport of solutes allowed us to identify the dominant controls on aquatic

https://doi.org/10.5194/egusphere-2026-2540
Preprint. Discussion started: 13 May 2026

carbon transformation and to improve predictions of how warming-induced permafrost change may alter coupled carbon and solute cycling in one of the largest Arctic river basins.

2. Study Site, Materials and Methods

2.1. Lena River and its tributaries

The Lena River basin has an extremely cold continental climate, with winter air temperatures frequently below −30 °C from December to February. Positive mean air temperatures are generally limited to a short thaw period of about five months (May–September). Winter precipitation is low and mostly stored as snow, whereas most annual precipitation occurs in summer, coinciding with peak biological activity and river discharge. Permafrost is predominantly continuous, with discontinuous and sporadic zones in the southern basin (Brown et al., 2002). Along the main stem, mean annual air temperature (MAAT) decreases northward from about −9 °C in the central basin to −13.3 °C in the north, while tributaries span a broader MAAT range from −4.7 to −15.9 °C. Mean annual precipitation in the northern basin is low, 200–250 mm yr^{-1} (Chevychelov and Bosikov, 2010), reinforcing strong runoff seasonality and snowmelt dominance.

The lithology of the Lena basin upstream of Yakutsk is highly diverse and includes Archean and Proterozoic crystalline and metamorphic rocks, Upper Proterozoic to Ordovician carbonate formations, Permo–Triassic volcanic rocks, and widespread Phanerozoic terrigenous silicate sedimentary units. This geological heterogeneity exerts a major control on riverine major ions, trace elements, and inorganic carbon. More detailed descriptions of basin landscapes, vegetation, and geology are available elsewhere (Rachold et al., 1996; Huh et al., 1999a, b; Huh and Edmond, 1999; Pipko et al., 2010; Semiletov et al., 2011; Kutscher et al., 2017; Ogneva et al., 2023; Juhls et al., 2020, 2025). Together, these climatic, permafrost, and lithological gradients provide the framework for interpreting spatial variability in solute export, greenhouse gas dynamics, and weathering regimes along the Lena River continuum and its tributaries.

https://doi.org/10.5194/egusphere-2026-2540
Preprint. Discussion started: 13 May 2026

2.2. Sampling strategy

In the middle and lower Lena (Yakutsk to Kysyr), peak annual discharge typically occurs in June and is mainly driven by rapid snowmelt across the permafrost-dominated basin. Sampling was conducted from 5 to 22 July 2022, shortly after peak flow, during the early post-freshet recession. At this stage, river levels remain high but hydrological conditions are more stable than during peak flood, allowing integration of basin-wide snowmelt inputs while reducing short-term variability linked to flood-wave propagation and bank erosion. July conditions also correspond to active-layer deepening and enhanced subsurface connectivity, which promote mobilization of solutes, dissolved inorganic carbon (DIC), dissolved organic carbon (DOC), and greenhouse gases from soils and permafrost-affected terrains.

During the campaign, we navigated ~1500 km aboard the research vessel *Merzlotoved*, from Yakutsk (62.15 °N) to Samoilov Island (72.38 °N) in the Lena Delta (Fig. 1A). A total of 33 sites were sampled along the main stem, together with two major tributaries (Aldan and Vilyui) and four smaller tributaries (Seen-Yurekh, Undyulyung, Byusyuttak, and Molodo). Regular stops at ~50 km intervals along the main channel enabled systematic sampling of major hydrochemical parameters and greenhouse gases (GHG) along the longitudinal river gradient. This transect design aimed to resolve changes in solute composition, carbon speciation, and CO_2 and CH_4 concentrations in relation to northward permafrost gradients, lithological transitions, and contrasting tributary inputs. At selected confluences, sampling was performed 200–500 m upstream of the mixing zone to obtain representative tributary water and avoid backwater and incomplete mixing effects. Longitudinal transect sampling is widely used to assess river water chemistry in large and climatically extreme basins (Huh and Edmond, 1999; Spence and Telmer, 2005). Sampling during the high-flow season also provides the closest agreement with annual flux estimates derived from time series, because this period accounts for a large share of annual water and solute export (Qin et al., 2006).

2.3. Hydrology and water surface area estimation

July corresponds to the high-flow period of the Lena River, representing the recession phase of the spring freshet. Although peak discharge typically occurs in June, river levels remain elevated in July

https://doi.org/10.5194/egusphere-2026-2540
Preprint. Discussion started: 13 May 2026

due to delayed snowmelt from northern and high-elevation sub-basins and continued active-layer development in permafrost-dominated terrains. Hydrographs for the studied large rivers were constructed using discharge data from the Automated Information System of the State Monitoring of Water Bodies (https://gmvo.skniivh.ru/). These time series were used to position the sampling campaign within the seasonal hydrograph and to assess deviations from long-term mean discharge during the sampling period. To characterize hydrological and geomorphological controls on river chemistry, watershed-scale parameters were calculated for each sampling point (Fig. 1A), including total watershed area, river network density, and total watercourse length. These parameters were derived from HydroSHEDS shapefiles (https://www.hydrosheds.org/) using standard GIS procedures.

Water surface area was quantified from Landsat 8–9 Level-2 surface reflectance products (Collection 2) acquired during 5–22 July 2022. Cloud-free scenes were atmospherically corrected, orthorectified, mosaicked, and processed in ArcGIS. Water bodies were delineated using the Normalized Difference Water Index (NDWI) and Modified NDWI (MNDWI), based on green, near-infrared, and shortwave infrared bands, with thresholds calibrated for Lena River conditions, including turbid waters. Classified rasters were converted to polygon shapefiles and manually corrected along shorelines, shallow areas, and zones affected by suspended sediments or aquatic vegetation. In total, 269 water polygons were identified. To improve area accuracy, polygons were subdivided using the Fishnet tool, and surface areas were calculated individually using planar geometry within appropriate WGS 84 / UTM projection zones. Delineation accuracy was visually checked against high-resolution imagery (e.g., Google Earth) and river morphology.

Water discharge at each sampling point and date was estimated from gauging-station data by linear interpolation and hydraulic scaling along the main stem and tributaries, accounting for incremental drainage area and tributary inflows. Surface water discharge, watershed area, river network length, and latitude (used as an integrative proxy of climatic and permafrost gradients) were then compared with surface-water chemistry to assess controls on dissolved major elements, trace elements, and carbon species.

https://doi.org/10.5194/egusphere-2026-2540
Preprint. Discussion started: 13 May 2026

2.2. CO_2 and CH_4 concentrations

Dissolved CO_2 in surface waters was measured in situ using a portable infrared gas analyzer (IRGA; GMT222 CARBOCAP® probe, Vaisala®; accuracy ±1.5%) operating in two ranges (0–2,000 and 0–10,000 ppm). The sensor was installed in the vessel's Kingston water intake system, where continuous flow (~20 L min^{-1}) ensured constant renewal of river water during navigation. For aqueous deployment, the probe was protected by a gas-permeable, waterproof expanded polytetrafluoroethylene (PTFE) membrane, which allows rapid CO_2 diffusion while preventing water intrusion (Johnson et al., 2009). A copper mesh was added to reduce potential biofouling (Yoon et al., 2016), although such effects were expected to be minimal in the cold, low-impacted Lena waters.

At each station, the sensor was equilibrated for ~10 min before measurement. CO_2 concentration (ppm), water temperature (°C), and atmospheric pressure (mbar) were logged every minute using a Campbell data logger during 5-min measurement sequences repeated every 30 min, yielding 153 individual records. For the main stem, values were averaged over three consecutive 5-min sequences, each representing ~1.25 km of river distance. At tributary confluences, measurements were performed 200–500 m upstream of the mixing zone. Sensors were calibrated before and after the expedition against certified gas standards (0, 800, 3,000, and 8,000 ppm), yielding linear relationships with $R^2 > 0.99$. Instrumental drift ranged from 0.03 to 0.06% d^{-1}, and post-processing corrections for temperature and pressure followed Johnson et al. (2009). Overall uncertainty of individual pCO_2 measurements was ≤10%.

Methane concentrations were determined from unfiltered water collected in 60 mL serum bottles without headspace, preserved with 0.2 mL saturated $HgCl_2$, and analyzed in the laboratory by headspace equilibration with ultra-high-purity N_2. Two 0.5 mL aliquots of the equilibrated headspace were measured on a Bruker GC-456 gas chromatograph equipped with flame ionization and thermal conductivity detectors. Calibration was performed every 10 samples using certified standards (Air Liquide; 145 ppmv), and duplicate injections showed reproducibility within ±5%. Dissolved CH_4 concentrations were calculated from headspace measurements using temperature-dependent solubility coefficients (Yamamoto et al., 1976) and mass-balance equations. Combined uncertainty of CH_4

https://doi.org/10.5194/egusphere-2026-2540
Preprint. Discussion started: 13 May 2026

concentrations was estimated at 7–12%. These analytical uncertainties are small relative to the observed spatial gradients in CO_2 and CH_4 and do not affect the interpretation of longitudinal and tributary-scale patterns.

2.3. Flux measurement and calculation

Diffusive CO_2 fluxes (F_{CO_2}) were measured using two floating chambers (ca. 30 cm diameter, ~10 L volume) equipped with non-dispersive infrared CO_2 sensors (SenseAir). Sensors were calibrated in the laboratory against certified N_2–CO_2 gas mixtures prior to field deployment. During measurements, chambers floated freely at the water surface, and headspace CO_2 was logged continuously over 5-min intervals. Fluxes were calculated from the initial linear accumulation phase using the first 30 min of deployment (Serikova et al., 2018; Vorobyev et al., 2024).

In addition to direct chamber measurements, diffusive CO_2 fluxes were independently estimated using the bulk gas exchange equation of Cai and Wang (1998):

$$F_{CO_2} = K_h \, k_{CO_2} \, (C_{water} - C_{air}) , \quad (1)$$

where K_h is the Henry's constant corrected for temperature and pressure (mol L^{-1} atm^{-1}), k_{CO_2} is the gas exchange velocity at a given temperature, C_{water} is the water CO_2 concentration, and C_{air} is the CO_2 concentration in the ambient air. Conversion between dissolved concentration and partial pressure followed Wanninkhof et al. (1992) and Lauerwald et al. (2015). Atmospheric CO_2 for July 2022 was taken as 417.9 ppm from the WMO global monitoring network, consistent with the nearest Tiksi station (422.5 ppm; https://community.wmo.int/wmo-greenhouse-gas-bulletins; https://www.meteorf.gov.ru/product/infomaterials/90/). Temperature-dependent solubility constants followed Wanninkhof et al. (1992).

A median gas transfer velocity of 4.46 m d^{-1} was adopted from measurements in four major Western Siberian rivers (Karlsson et al., 2021), consistent with previous estimates for the Lena River (Vorobyev et al., 2021a), the Kolyma (Denfeld et al., 2013), the Yukon (Striegl et al., 2012), and global syntheses for large rivers (Alin et al., 2011; Raymond et al., 2013). Wind speeds during sampling were

https://doi.org/10.5194/egusphere-2026-2540
Preprint. Discussion started: 13 May 2026

below 3.7 m s^{-1} and water surfaces were visually smooth, supporting the use of this literature-constrained K_T value (Jähne et al., 1987; Alin et al., 2011; Guérin et al., 2007).

Instantaneous diffusive CH_4 fluxes were calculated using an equation analogous to Eq. (1), with gas transfer velocities derived from chamber-measured CO_2 fluxes and in situ CO_2 concentrations, following approaches used for Western Siberian rivers (Serikova et al., 2018; Lim et al., 2022; Vorobyev et al., 2024). Dissolved CH_4 concentrations were combined with atmospheric equilibrium concentrations assuming a background atmospheric pCH_4 of 1.8 ppm and the 2022 mean atmospheric CH_4 concentration from Mauna Loa Observatory (http://aftp.cmdl.noaa.gov/products/trends/ch4/ch4_annmean_gl.txt), following Serikova et al. (2018, 2019). Flux uncertainty was dominated by variability in gas transfer velocity rather than by analytical uncertainty in dissolved gas concentrations. Concentration uncertainty contributed comparatively little (≤10% for CO_2 and 7–12% for CH_4), whereas kkk may vary by ±40–60% depending on hydraulic conditions (Raymond et al., 2013). Sensitivity analysis showed that using a conservative kkk value of 3 m d^{-1} instead of 4.46 m d^{-1} would decrease calculated CO_2 emissions by about 30%, while preserving the spatial patterns along the transect. Because the objective of this study is to resolve relative gradients between tributaries and main-stem sections rather than derive absolute annual budgets, the adopted kkk parameterization provides a robust and internally consistent basis for comparative flux analysis.

2.4. Physicochemical parameters and laboratory analyses

In situ dissolved oxygen, specific conductivity, and water temperature were measured at ~20 cm depth using a WTW 3320 multimeter equipped with a CellOx 325 oxygen probe (±5%), a TetraCon 325 conductivity sensor (±1.5%), and a temperature sensor (±0.2 °C). pH was measured with a portable Hanna instrument fitted with a combined Schott glass electrode, calibrated daily with NIST-traceable buffers (pH 4.01, 6.86, and 9.18 at 25 °C), yielding an uncertainty of ±0.01 pH units. Buffer temperatures were kept within ±5 °C of river water temperature.

Surface water was collected from 20–30 cm depth near the channel center into pre-cleaned polypropylene bottles and immediately filtered through sterile single-use Sartorius filters (0.45 µm). The

https://doi.org/10.5194/egusphere-2026-2540
Preprint. Discussion started: 13 May 2026

first 50 mL of filtrate were discarded. Milli-Q blanks confirmed negligible DOC contamination from the filters. Filtered samples were split into aliquots: one was acidified to 2% (v/v) with bidistilled HNO_3 in pre-cleaned polypropylene vials for major and trace element analyses; the second, non-acidified fraction was used for DOC, DIC, and UV absorbance. Samples were stored at 4 °C and analyzed within 30 days. DOC and DIC were measured with a Shimadzu TOC-VSCN analyzer (detection limit 0.1 mg L^{-1}; precision ±3%). Nutrients were analyzed on frozen filtered samples by ion chromatography (Dionex ICS-5000+) with ±2% uncertainty; certified reference materials Ion-915 and Ion-964 were within 10% of certified values. Major and trace elements were determined in acidified samples by ICP-MS (Agilent 8500ce, Ar and He modes). Precision ranged from 5–10% at 1–1000 µg L^{-1} to 10–20% at 0.001–0.1 µg L^{-1}. Accuracy and reproducibility were checked using SLRS-6 and three in-house multi-element standards every 20 samples (Yeghicheyan et al., 2019), with agreement within 10–15% for 40 elements.

Ten selected samples were additionally processed by dialysis (1 kDa cutoff) to distinguish low-molecular-weight (<1 kDa) and colloidal (1 kDa–0.45 µm) fractions. River water was pre-screened through a 20 µm nylon mesh and placed in cleaned 5 L polyethylene containers; pre-cleaned 50 mL dialysis bags were immersed for 3–5 days following established procedures (Vasyukova et al., 2010; Pokrovsky et al., 2016b; Kolesnichenko et al., 2021). Containers were kept dark at near in situ temperature and gently agitated. Dissolved solute concentrations before and after dialysis differed by <10% ($p < 0.01$), indicating negligible alteration of dissolved and colloidal composition during incubation.

Total bacterial cell concentration (TBC) was measured by flow cytometry after fixation with glutaraldehyde, following Marie et al. (1999).

2.5. Statistical treatment of the data

Depending on data distribution, Pearson correlation coefficients were calculated to assess linear relationships between variables, and statistical significance was evaluated at $p < 0.05$. To further identify the dominant drivers of dissolved carbon variability (CO_2, DIC, and DOC), multivariate statistical analysis was performed using Principal Component Analysis (PCA). This approach allowed us to assess

https://doi.org/10.5194/egusphere-2026-2540
Preprint. Discussion started: 13 May 2026

the combined influence of hydrochemical parameters (major ions, nutrients, trace elements), hydrological variables (discharge, watershed area), and climatic factors (e.g., latitude as an integrative proxy) on spatial patterns of dissolved carbon in river waters. Prior to PCA, all variables were standardized to zero mean and unit variance to eliminate bias related to differences in measurement units and value ranges. The analysis was performed using STATISTICA 7 (StatSoft Inc., http://www.statsoft.com). Principal components were extracted from the raw data matrix using the covariance structure of standardized variables.

The number of significant components was determined using a scree plot analysis, where eigenvalues were plotted in descending order against component number. A pronounced decrease in eigenvalues between the first (F1) and second (F2) components indicated that the majority of explained variance was captured by the first two factors. Consequently, only these two principal components were retained for interpretation.

3. Results

3.1. Hydrological parameters

Hydrograph analysis (**Fig. 1 B**) indicates that river discharge during the study period was primarily sustained by groundwater contributions and rainfall inputs following the spring snowmelt peak. By July, the Lena River was in the recession phase of the freshet, characterized by gradually declining but still elevated discharge sustained by subsurface flow and delayed runoff from northern and high-latitude sub-basins. The estimated water travel time between the upstream gauging station at Tabaga and the downstream station at Kyusur was approximately 12 days under the observed hydrological conditions. This relatively short transit time implies efficient downstream propagation of water masses and associated solutes along the main stem during high-flow conditions.

The drainage network of the Lena basin is well developed, with a mean river network density of 0.22 km km^{-2}. According to Strahler's classification, stream order within the basin ranges from first-order headwater streams to ninth-order channels along the main stem, reflecting the hierarchical organization and large spatial integration of tributary inputs. Hydrologically, 2022 corresponded to a

https://doi.org/10.5194/egusphere-2026-2540
Preprint. Discussion started: 13 May 2026

relatively high-flow year when compared to long-term records prior to the 1970s. Mean annual discharge reached 10,501 $m^3 s^{-1}$ at Tabaga and 19,745 $m^3 s^{-1}$ at Kyusur, placing 2022 among the upper range of historical values. However, in the context of the past two decades, these values fall within the range of average annual discharge reported by the Russian Federal Service for Hydrometeorology and Environmental Monitoring (Roshydromet), consistent with recent assessments (Juhls et al., 2025). Thus, while elevated relative to early historical records, hydrological conditions during the expedition were representative of contemporary flow regimes in the Lena River. The combination of high discharge, rapid downstream water transit (~12 days), and strong tributary integration created conditions favorable for efficient longitudinal transport of dissolved carbon species and greenhouse gases, setting the framework for interpreting spatial gradients in CO_2, CH_4, DIC, DOC, and associated emission fluxes.

3.2. Dissolved carbon species and greenhouse gases along the Lena continuum

Under the elevated but hydrologically representative discharge conditions of July 2022, the Lena River system provides an opportunity to evaluate how basin-wide connectivity, tributary integration, and northward climatic gradients regulate dissolved carbon pools and greenhouse gas dynamics. Below, we describe the spatial distribution of pCO_2, CH_4, DIC, and DOC along the main stem and tributaries, and quantify associated diffusive carbon fluxes.

The principal hydrochemical carbon parameters of the Lena River main stem (pCO_2, CH_4, pH, O_2, E.C., DIC, and DOC) are summarized in **Table 1**. Along the main stem, concentration of DIC increased by a factor of 1.5 from south to north (**Fig. 2 A**) whereas DOC did not exhibit any systematic longitudinal trends (**Fig. 2 B**). Mean concentrations were 8.4 ± 2.7 mg L^{-1} for DOC and 7.5 ± 2.7 mg L^{-1} for DIC. These values are consistent with previous observations during summer baseflow conditions, when DOC concentrations averaged around 5 mg L^{-1} (range 2–12 mg L^{-1}; Cauwet and Sidorov, 1996; Lara et al., 1998; Lobbes et al., 2000; Kuzmin et al., 2009; Kutscher et al., 2017). Similarly, DIC concentrations are comparable to reported summer values (~10 mg L^{-1}; range 5–50 mg L^{-1}) and agree with measurements from Yakutsk in July (Sun et al., 2018; Juhls et al., 2025). These values are also consistent with measurements carried out in late August-early September 1995 a shipboard investigation

https://doi.org/10.5194/egusphere-2026-2540
Preprint. Discussion started: 13 May 2026

along a 1700 km section from Yakutsk to Stolb Island - beginning of the Lena Delta: average concentrations of DOC and DIC were around 7 and 10 mg L^{-1} , respectively (Semiletov et al., 2011).

Discrete pCO_2 measurements along the main stem indicated a weak northward decrease (**Fig. 2 C**). The mean pCO_2 during July 2022 was 1020 ± 420 µatm (median 892 µatm; range 600–2600 µatm), exceeding values previously reported for the lower Lena during late summer. For example, Semiletov (1999) and Semiletov et al. (2011) reported an average pCO_2 of 538 ± 96 µatm (range 380–727 µatm) for August–September 1995, while Pipko et al. (2010) measured 559 µatm in July 2003. Thus, pCO_2 levels during the present study were approximately twofold higher than earlier late-summer assessments. Floating chamber measurements yielded CO_2 fluxes (FCO_2) ranging from 0.11 to 0.82 g C–CO_2 m^{-2} d^{-1} along the main stem (**Fig. 2 D**). Using measured pCO_2 values and a literature-constrained gas transfer velocity of 4.46 m d^{-1} (Karlsson et al., 2021; Vorobyev et al., 2021a), CO_2 fluxes were calculated along the entire studied main stem (1153 km). Estimated fluxes ranged from near-zero or slightly negative values (atmospheric uptake in the Aldan River) to between 0.1 and 1.3 g C m^{-2} d^{-1} in most main stem and tributary sections (**Fig. 2 D**).

Methane concentrations in the main stem were low (mean 0.22 µmol L^{-1}; median 0.08 µmol L^{-1}) and displayed no significant longitudinal trend (**Fig. 2 E**). These values closely match CH_4 concentrations reported during the spring flood in the upper and middle Lena (0.059 ± 0.006 µmol L^{-1}; interquartile range 0.025–0.199 µmol L^{-1}; Vorobyev et al., 2021) and are also consistent with data from the lower Lena (0.03–0.085 µmol L^{-1}; Bussmann, 2013). With the exception of one floodplain lake sample—characterized by both elevated pCO_2 and CH_4—no systematic difference was observed between the main stem and tributaries (**Table S1**). As previously reported (Vorobyev et al., 2021), CH_4 concentrations were approximately 100-500 times lower than CO_2 concentrations. Consequently, diffusive CH_4 emissions accounted for less than 0.5% of total carbon emissions (**Fig. 2 F**) and are not further considered in the overall catchment-scale carbon budget.

When continuous pCO_2 measurements along the main stem (153 individual data points, with mean distance of 7.25 km) are examined along the south–north transect together with discrete observations from tributaries (**Fig. 3 A**), major tributary confluences emerge as clear discontinuities in

https://doi.org/10.5194/egusphere-2026-2540
Preprint. Discussion started: 13 May 2026

the longitudinal pattern. These zones are characterized by abrupt increases or decreases in CO_2 concentration, reflecting the input of waters with contrasting biogeochemical signatures. A similar pattern is observed for calculated continuous CO_2 fluxes (**Fig. 3 B**). The Vilyui River exhibited the highest emissions (up to 1.3 g C–CO_2 m^{-2} d^{-1}), highlighting its role as a major localized source of CO_2 to the main stem. In contrast, the Aldan River acted as a weak net CO_2 sink during the sampling period, indicating substantial spatial variability in tributary influence. Despite this pronounced local heterogeneity, the main stem displayed relatively stable bulk carbon characteristics. DOC concentrations remained spatially uniform, and DIC showed only a weak longitudinal trend, whereas pCO_2 and FCO_2 exhibited dynamic variability controlled by tributary inputs and in-stream processes. As a result, the Lena River functioned as a persistent net source of CO_2 to the atmosphere during July 2022. In contrast, CH_4 concentrations were low and spatially invariant, contributing only marginally to total carbon emissions. This pattern further supports the decoupling between bulk dissolved carbon pools and CO_2 evasion, with tributaries acting as primary modulators of short-scale variability along the river continuum.

3.3. Areal emission from the Low Lena River basin

Previous assessments of areal CO_2 emissions from lotic waters of the Lena River basin (Vorobyev et al., 2021a) were based on estimates of total river surface coverage for the entire watershed (28,197 km^2 in 2016, including 5,022 km^2 of seasonal water; Global SDG database). This estimate agrees well with the Global River Widths from Landsat (GRWL) Mask database value of 22,479 km^2. In contrast, the present study focuses specifically on the Low Lena sector, between Yakutsk and Kyusur (1,551,445 km^2 land area), encompassing 12,904 km^2 km^2 of water surface including the main stem (7529 km^2) and the two largest tributaries, the Aldan and the Vilyui (2377 and 2998 km^2, respectively).

For emission calculations, we adopted conservative summer baseflow conditions corresponding to the hydrological period of our expedition. Earlier work on Lena basin carbon emissions (Vorobyev et al., 2021) identified a major uncertainty in regional flux estimates due to the absence of direct pCO_2 measurements over ~1000 km of the northern main stem downstream of the Aldan confluence, including

https://doi.org/10.5194/egusphere-2026-2540
Preprint. Discussion started: 13 May 2026

the large Vilyui tributary. The present dataset fills this gap through continuous in situ pCO_2 measurements and direct chamber-based flux determinations in this hydrologically and climatically sensitive section of the basin. During the spring flood, the Aldan River—contributing up to 70% of Lena discharge during peak freshet (Pipko et al., 2010)—was previously reported as a strong CO_2 source (3.2 ± 0.5 g C m^{-2} d^{-1}), compared to 1.69 ± 0.08 g C m^{-2} d^{-1} upstream of the confluence (Vorobyev et al., 2021). In contrast, during July 2022, the Aldan did not act as a significant CO_2 emitter (measured FCO_2 = –0.03 µmol m^{-2} s^{-1}; pCO_2 = 1014 µatm), indicating strong seasonal contrasts in carbon evasion dynamics. Conversely, the Vilyui River exhibited the highest chamber-measured emissions (1.3 g C m^{-2} d^{-1}; pCO_2 = 1340 µatm), exceeding main-stem values by more than a factor of three. Note that calculated fluxes for these two tributaries were much more similar, amounting to 0.31 and 0.485 g C m^{-2} d^{-1}, respectively.

For areal emission calculations along the main stem, we used the chamber-derived mean CO_2 flux of 0.33 ± 0.20 g C m^{-2} d^{-1} (n = 12) measured along the south–north transect. By comparison, fluxes calculated from continuous and discrete pCO_2 measurements (mean 957 ± 230 µatm, n = 153) using a gas transfer velocity of K_T = 4.46 m d^{-1}—consistent with previous applications to large Siberian rivers (Karlsson et al., 2022; Vorobyev et al., 2021a)—yielded nearly identical values (0.32 ± 0.20 g C m^{-2} d^{-1}). The experimentally derived piston velocity obtained from paired chamber flux and pCO_2 measurements averaged K_T = 8.82 ± 6.76 m d^{-1}, indicating spatially variable and locally enhanced gas exchange conditions in the Low Lena reaches. Such elevated values likely reflect periods of increased turbulence associated with strong northerly winds aligned with the main river channel, producing long fetch and enhanced surface mixing. Despite this variability, the agreement between chamber-derived fluxes and those calculated using $K_T \approx 4$ m d^{-1} suggests that the globally averaged gas transfer velocity proposed by Raymond et al. (2013), and applied in previous studies of large Siberian rivers (Karlsson et al., 2022; Vorobyev et al., 2021a), provides a reasonable and robust approximation for estimating CO_2 emissions from the lower Lena River.

Therefore, for basin-scale calculations, we adopted fluxes derived using a gas transfer velocity of K_T = 4.464 m d^{-1}, consistent with chamber-constrained estimates and representative of the full variability observed along the main stem between Yakutsk and Kyusur (**Fig. 2 C, D** and **Fig. 3**). Emission estimates

https://doi.org/10.5194/egusphere-2026-2540
Preprint. Discussion started: 13 May 2026

were area-weighted by accounting for the relative water surface occupied by the main stem (58% of the total Low Lena water area) and by incorporating the contributions of the two largest tributaries, the Vilyui and Aldan Rivers, which represent 23% and 18% of the total water surface area, respectively. The resulting water-area-weighted CO_2 emission estimate for the Low Lena during the transition from the end of the spring flood to the onset of baseflow equals 0.36 ± 0.15 g C m^{-2} d^{-1}. These revised emission estimates, constrained by direct chamber measurements and hydrodynamic adjustment of gas transfer velocity, provide a refined carbon budget for the Low Lena and set the stage for examining how spatial variability in major and trace solutes reflects the lithological, hydrological, and permafrost controls underlying these carbon dynamics.

3.4. Spatial pattern of major and trace solutes

All measured hydrochemical parameters for the Low Lena River and its tributaries are reported in Table S1 (Supplementary Excel file). Based on longitudinal trends along the main stem, three principal groups of solutes were identified: (*i*) Low-solubility trivalent and tetravalent elements and strong hydrolysates, exhibiting a significant northward decrease in concentration (**Fig. 4**). This group includes Al, Sc, Ga, Y, rare earth elements (REEs), Ti, Th, U, Be, and Nb. These elements are typically associated with particulate or colloidal phases and display conservative removal or dilution along the river continuum. (*ii*) Labile major cations and anions (including carbonate-related species), showing increasing concentrations from south to north (**Fig. 5**). This group comprises DIC, SO_4^{2-}, B, Mg, P, Ca, Sr, As, Se, and Sb, consistent with progressive downstream integration of groundwater inputs and lithological controls. (*iii*) Components without statistically significant longitudinal trends, defined by correlation coefficients $|r| < 0.3$ ($p > 0.05$) with the latitude (**Table S2**). This category includes DOC, greenhouse gases (CO_2 and CH_4), major anions (Cl^-, F^-, NO_3^-), Si, K, V, Cr, Mn, Fe, Ni, Cu, Zn, Co, Cd, Rb, Mo, Cs, Ba, Hf, W, Tl, Pb, and Bi. These solutes exhibited spatial variability but no systematic south–north gradient along the main channel.

In addition to longitudinal patterns, distinct local anomalies were observed in certain tributaries. For example, Mn concentrations in the Undyulyung River (LIV 17) exceeded adjacent main-stem values

https://doi.org/10.5194/egusphere-2026-2540
Preprint. Discussion started: 13 May 2026

by a factor of 27. Similarly, Fe and Mn concentrations in the Byusyuttakh and Molodo tributaries (LIV 28 and LIV 29) were elevated relative to the main channel by factors of approximately 2 and 5, respectively. However, such deviations were not widespread. For most elements, concentrations in tributaries were comparable to those measured in neighboring main-stem sections, typically within ±30% of adjacent values. This overall similarity indicates efficient mixing and strong integration of tributary inputs within the large-channel hydrodynamic framework of the Low Lena. The contrasted longitudinal behavior of solutes reflects the superposition of at least two first-order controls along the Low Lena continuum: (*i*) progressive hydrological integration and groundwater contributions enhancing mobile, carbonate-related species (DIC, Ca, Mg, Sr, SO_4^{2-}), and (*ii*) downstream dilution and/or sedimentation of low-solubility hydrolysates and colloid-associated trivalent–tetravalent elements (Al, REEs, Ti, Th, U). In contrast, the majority of elements and DOC displayed spatial variability without a systematic northward gradient, suggesting compensation between source inputs, in-stream processing, and hydrodynamic mixing within the large-channel system.

3.5. Correlations and multiparametric treatment

Multivariate statistical treatment was restricted to the Lena main stem (n = 27), as the number of sampled tributaries (n = 6) was insufficient for robust statistical analysis. Pairwise Pearson correlation analysis revealed several significant ($p < 0.05$) relationships among dissolved constituents. pCO_2 showed positive correlations with labile major ions, including F^-, Cl^-, and Na^+, suggesting linkage to water–rock interaction and/or groundwater inputs. Diffusive CO_2 flux was positively correlated with DOC (R^2 = 0.40; **Fig. 6 A**), nutrients (P, K), and selected trace metals (V, Ni), as listed in **Table S2**. In contrast, CH_4 concentrations did not exhibit statistically significant correlations with any measured hydrochemical parameter. DIC concentrations correlated positively with mobile anions (e.g., Br^-), nutrients (Si, P, Rb), and redox-sensitive or labile oxyanions such as As, with a strong linear relationship shown in **Fig. 6 B**. Aluminum, representing low-solubility lithogenic elements, displayed strong positive correlations with trivalent and tetravalent hydrolysates including Ti, Ga, Y, and REEs (**Fig. 6 C, D**), and to a lesser extent

https://doi.org/10.5194/egusphere-2026-2540
Preprint. Discussion started: 13 May 2026

with Th and U. These relationships indicate a shared lithogenic origin and likely transport in colloidal or fine particulate form.

To further disentangle the structure of covariation among solutes, Principal Component Analysis (PCA) was applied to the standardized dataset. Two principal components explained 23% and 13% of the total variance, respectively (**Fig. 7; Table S3**). The first factor (F1) was positively loaded on lithogenic, low-solubility elements including Be, Al, Ti, Ga, Y, Nb, REEs, and Th, consistent with a common refractory mineral source and transport via colloidal phases (see next Section 3.6). This factor exhibited negative loadings for highly soluble and mobile constituents such as B, SO_4^{2-}, DIC, Mg, and Sr, suggesting an opposing control linked to groundwater connectivity and carbonate weathering inputs. The second factor (F2) primarily captured latitudinal variability and was associated with DOC, labile nutrients (P, K, V, Mo), and several mobile trace elements (Co, Ni, As, Sb, Cs), but also included refractory elements such as Sc, Zr, and Hf. This mixed loading pattern indicates combined influence of surface-derived sources (e.g., plant litter leaching and soil organic matter mobilization) and lithogenic contributions, potentially mediated by interaction with suspended particulate matter, as previously observed in other Siberian river systems (Kolesnichenko et al., 2022; Lim et al., 2024). Notably, a comparable PCA structure—distinguishing lithogenic/colloidal elements from soluble weathering-derived constituents—was reported for the upper and middle Lena during peak spring flood conditions (Vorobyev et al., 2021), suggesting persistent large-scale controls on solute organization across hydrological seasons. The strong covariation among low-solubility lithogenic elements identified by correlation and PCA analyses suggests a dominant role of colloidal transport; this hypothesis is directly evaluated below using operational size-fractionation by dialysis.

3.6. Colloidal Status of Major and Trace Elements in the Lena River and Tributaries

Dialysis (1 kDa cutoff) enabled operational separation of nominal low-molecular-weight ($LMW_{<1\ kDa}$) and colloidal (1 kDa–0.45 µm) fractions within the dissolved pool (<0.45 µm). The colloidal proportion of each element was calculated as the percentage of its concentration in the 1 kDa–0.45 µm fraction relative to its total dissolved concentration (< 0.45 µm). Across the northern Lena basin, the

https://doi.org/10.5194/egusphere-2026-2540
Preprint. Discussion started: 13 May 2026

relative contribution of colloidal forms was remarkably consistent between the main stem and tributaries (**Fig. 8**). The colloidal fraction ranged from negligible values (0–10%) for highly soluble species such as DIC, Li, and Si, to dominant proportions (80–90%) for trivalent and tetravalent hydrolysates. Based on colloidal abundance, three principal groups of solutes were distinguished: (1) Predominantly truly dissolved species (0–20% colloidal fraction): Alkali and alkaline-earth metals (Li, Na, K, Rb, Mg, Ca, Sr), major inorganic carbon (DIC), Si, and selected trace oxyanions (Mo, As). These elements are largely present in low-molecular-weight forms and exhibit minimal association with colloidal phases. (2) Mixed LMW–colloidal species (20–60% colloidal fraction): P, Al, and several trace metals (Cu, V, Sc, Ni, Cr, Co, U) showed intermediate colloidal contributions. Dissolved organic carbon (DOC) exhibited a mean colloidal proportion of 41 ± 14%, indicating that a substantial fraction of riverine organic carbon is associated with supramolecular or organo-mineral colloidal structures. (3) Predominantly colloidal elements (80–90% colloidal fraction): Certain divalent metals (Mn, Ba, Zn, Pb) and refractory lithogenic hydrolysates (Fe, Ga, Y, REEs, Ti, Zr, Hf, Th, Be, Nb) were largely transported in colloidal form, consistent with strong hydrolysis tendencies and association with Fe- and Al-rich mineral or organo-mineral particles. No major difference in colloidal partitioning was observed between the main stem and tributaries. In particular, DOC exhibited a remarkably uniform colloidal proportion (41 ± 14%) across the main stem and four tributaries, including the largest ones (Vilyui and Aldan). The only notable deviation occurred in a floodplain lake hydrologically disconnected from the main channel, where DOC, Al, and Co displayed 20–30% higher colloidal fractions relative to fluvial waters. Overall, the Lena River system exhibited a highly structured and spatially homogeneous colloidal organization, with refractory lithogenic elements transported predominantly in colloidal form, mobile weathering-derived solutes remaining largely truly dissolved, and DOC occupying an intermediate and remarkably stable colloidal niche across the basin.

https://doi.org/10.5194/egusphere-2026-2540
Preprint. Discussion started: 13 May 2026

4. DISCUSSION

The Low Lena River during the post-freshet high-flow period exhibits a structured but internally consistent hydrobiogeochemical organization. While bulk dissolved carbon pools (DOC and DIC) remain relatively stable along the main stem, CO_2 persists in a state of supersaturation, sustaining moderate but spatially variable atmospheric evasion. In parallel, major and trace solutes segregate into distinct longitudinal patterns: mobile weathering-derived species progressively increase downstream, low-solubility lithogenic hydrolysates decline, and the majority of redox-sensitive and nutrient elements show no systematic gradient. Multivariate statistics and size-fractionation analyses further demonstrate that this organization is governed by the interplay of groundwater connectivity, lithological control, and colloidal transport, which together regulate both dissolved carbon dynamics and trace-element mobility. Below, we place these observations into the broader context of Arctic river biogeochemistry and evaluate the mechanisms controlling solute and greenhouse gas transport in the Low Lena basin.

4.1. Latitudinal pattern of dissolved C in the Low Lena River basin

The chamber-derived CO_2 emissions measured along ~800 km of the Low Lena main stem (0.1–1.3 g C m^{-2} d^{-1}) fall within the lower range of values previously reported for large Arctic and boreal rivers. The resulting water-area-weighted CO_2 emission estimate for the Low Lena during the transition from the end of the spring flood to the onset of baseflow equals 0.36 ± 0.15 g C m^{-2} d^{-1} (range 0.1 to 1.3 g C m^{-2} d^{-1}) which is substantially lower than the 1.65 ± 0.5 g C m^{-2} d^{-1} (range 0.8 to 1.7 g C m^{-2} d^{-1}) previously reported for the upper and middle Lena during peak freshet (Vorobyev et al., 2021). This seasonal difference likely reflects shifts in dominant metabolic and hydrological processes. During peak snowmelt, large inputs of CO_2-rich soil and groundwater promote strong supersaturation and enhanced outgassing. In contrast, later in the season, reduced lateral inputs combined with increasing in-stream primary production, partial CO_2 uptake by photosynthesis, and degassing along the river continuum may collectively decrease the net areal CO_2 flux.

https://doi.org/10.5194/egusphere-2026-2540
Preprint. Discussion started: 13 May 2026

The emissions of Low Lena main stem and tributaries during this period are also below those reported for the Ob River main channel in permafrost-free regions (1.32 ± 0.14 g C m^{-2} d^{-1}; Karlsson et al., 2021), small rivers within the continuous permafrost zone of western Siberia (0.98 g C m^{-2} d^{-1}; Serikova et al., 2018), and the Low Ob River during spring flood peak (1.56 ± 0.47 g C–CO_2 m^{-2} d^{-1}; Vorobyev et al., 2024). At the same time, Lena's fluxes are very similar to those of the Kolyma River main stem (0.35 g C m^{-2} d^{-1}; Denfeld et al., 2013). Thus, under post-freshet summer conditions, the Low Lena behaves as a moderate but persistent CO_2 source to the atmosphere, consistent with the broader Arctic riverine carbon paradigm.

As previously documented for the upper and middle Lena during peak spring discharge (Vorobyev et al., 2021), pCO_2 along the main stem exhibited marked short-distance variability (**Fig. 3 A**), reflecting the interplay of external inputs and in-stream processing. Tributary inflows with contrasting CO_2 signatures are widely recognized as primary drivers of spatial heterogeneity in Arctic river systems (Crawford et al., 2013; Leith et al., 2014, 2015; Hotchkiss et al., 2015; Dean et al., 2020; Vonk et al., 2023). Superimposed on this lateral variability, internal riverine processes—including turbulence-controlled gas exchange (Raymond et al., 2013; Rocher-Ros et al., 2023), sediment resuspension and benthic respiration (Hopkinson, 1985; Humborg et al., 2010), and mineralization of organic carbon in the water column (Cole et al., 2007; Attermeyer et al., 2018)—can modify CO_2 concentrations over short spatial scales. In permafrost-dominated catchments, additional variability arises from lateral inflow of CO_2-rich suprapermafrost waters derived from thawed active layers and shallow groundwater pathways (Bagard et al., 2011; Vonk et al., 2015; Raudina et al., 2018; Vorobyev et al., 2024; Krickov et al., 2026). Given that our measurements were averaged over ~1.5 km segments, the observed fluctuations cannot be attributed to analytical noise but instead reflect genuine spatial heterogeneity in CO_2 dynamics along the main channel.

Among all dissolved carbon variables, only pCO_2 displayed a statistically significant latitudinal pattern, decreasing from south to north. This gradient likely reflects a combination of interacting controls. First, southern reaches receive substantial contributions from the Aldan and Vilyui tributaries, whose watersheds encompass extensive forested and more productive landscapes, promoting higher terrestrial

https://doi.org/10.5194/egusphere-2026-2540
Preprint. Discussion started: 13 May 2026

CO_2 inputs. Second, vegetation density and soil organic carbon stocks generally decline northward, potentially reducing lateral CO_2 supply from soils. Third, progressive hydrological disconnection between soil water and the river network toward the delta, together with increased channel width and reduced turbulence, may enhance degassing efficiency and decrease downstream pCO_2. Collectively, these factors suggest that the south-to-north decline in pCO_2 integrates shifts in terrestrial carbon supply, tributary influence, and hydrodynamic processing along the Low Lena continuum.

Notably, the spatial behavior of pCO_2 is largely decoupled from that of bulk dissolved carbon pools. Neither DOC nor DIC exhibited significant longitudinal trends ($R^2 < 0.18$), whereas pCO_2 declined systematically northward ($R^2 > 0.52$) and showed pronounced local variability. This pattern indicates that CO_2 supersaturation in the Lena main stem is not directly governed by total dissolved carbon concentration but rather by the balance between production, lateral supply, and evasion processes. In large Arctic rivers, DIC represents an integrated signal of carbonate weathering, groundwater inputs, and in-stream carbon transformations, while pCO_2 responds more sensitively to short-term respiration, suprapermafrost inflows, and hydrodynamic degassing (Mu et al., 2025). The absence of a clear coupling between DOC or DIC concentrations and pCO_2 therefore suggests that CO_2 dynamics are controlled primarily by process rates and hydrological connectivity rather than by the standing stock of dissolved carbon. Such functional decoupling between carbon pools and gas supersaturation has been increasingly recognized in high-latitude river systems, where rapid lateral exchange and efficient degassing can maintain relatively stable DOC and DIC concentrations despite substantial CO_2 evasion (Crawford et al., 2013; Karlsson et al., 2021; Vorobyev et al., 2024). In summary, while DOC and DIC remain relatively uniform along the Low Lena main stem, CO_2 exhibits pronounced local variability and a coherent latitudinal decrease, indicating that atmospheric evasion in this large Arctic river is primarily controlled by spatial heterogeneity in terrestrial inputs and hydrodynamic processing rather than by bulk dissolved carbon concentrations alone. To place these latitudinal carbon dynamics into a broader geochemical context, it is essential to discuss other solute concentrations and compare them with long-term monitoring records and to evaluate the mechanisms governing major and trace element export in the Low Lena basin.

https://doi.org/10.5194/egusphere-2026-2540
Preprint. Discussion started: 13 May 2026

4.2. Comparison with Other Data on Element Concentration in the Lena River and its Tributaries, Possible Carriers and Mechanisms of Major and Trace Solute Export

4.2.1. Long-term consistency of major solutes and comparison with recent spatial surveys

Several datasets document major solute concentrations in the Lena main stem during summer baseflow. The concentrations of major solutes measured in the present study (Na, Cl, Si, Ca, Mg, SO_4, DIC) agree within 30% with values reported for the Yakutsk–Kyusur sector during July–August (Kuzmin et al., 2009; Juhls et al., 2020). Similarly, comparison with long-term hydrochemical monitoring at the Kyusur gauging station (Gordeev and Sidorov, 1993), as well as more recent datasets from the PARTNERS and ARCTIC GRO programs (Cooper et al., 2008; Holmes et al., 2012; McClelland et al., 2015; Gordeev et al., 2024) and high-frequency sampling at Samoylov Island (Juhls et al., 2025), demonstrates agreement within 20–30% for Si, SO_4, Cl, F, Ca, K, Mg, Na, Al, Mn, and Sr at the northernmost sampling points. Fe concentrations measured here were approximately two times higher, whereas NO_3 concentrations were up to six times lower than previously reported. These deviations may reflect local redox conditions, biological uptake, and space- and seasons-dependent partitioning of Fe between colloidal and particulate phases (Hirst et al., 2020).

The most spatially extensive recent surveys of the lower Lena north of Yakutsk were conducted by Swedish research teams (Murphy et al., 2018; Sun et al., 2018; Hirst et al., 2017, 2020; Mavromatis et al., 2024). Dissolved concentrations of Li, Na, K, Mg, Si, Al, and Fe measured in this study fall within the ranges reported for July–August conditions by these authors. This agreement across independent expeditions underscores the reproducibility of Lena hydrochemistry during the open-water season and suggests that contemporary climatic warming has not yet induced drastic shifts in bulk solute export during summer baseflow. Variability in most solutes rarely exceeded a factor of 2–3, reinforcing the view that the Low Lena behaves as a hydrologically integrated and chemically buffered system during this period. Overall, the consistency across datasets spanning more than five decades and ~800 km of the main stem indicates remarkable temporal and spatial stability of major solute concentrations during summer baseflow conditions. Such stability is characteristic of large Arctic rivers where deep groundwater inputs and basin-scale integration of surface flux buffer short-term variability.

https://doi.org/10.5194/egusphere-2026-2540
Preprint. Discussion started: 13 May 2026

4.2.2. Colloidal carriers and trace element mobility

Dissolved organic matter and DOM-stabilized Fe and Al oxyhydroxides are widely recognized as dominant colloidal carriers of trace elements in boreal and permafrost-affected humic waters (Loiko et al., 2017; Raudina et al., 2021; Stolpe et al., 2013a,b; Cuss et al., 2017, 2018, 2020; Vasyukova et al., 2010; Ilina et al., 2016). Although based on a limited number of dialysis samples, our results confirm that low-solubility trivalent and tetravalent hydrolysates, as well as U, Cr, V, Pb, Mn, Zn, and Ba, are predominantly transported in the colloidal (1 kDa–0.45 µm) fraction.

Pairwise correlations further reveal two distinct geochemical associations. Nutrients and relatively labile metals (Si, P, Li, K, Rb, V, Ni, Cu) correlate strongly with DOC, suggesting common mobilization from organic-rich surface soils and plant litter followed by lateral transport along the hydrological continuum (Krickov et al., 2026). In contrast, Al correlates with refractory lithogenic elements (Ti, Y, REEs), consistent with mobilization from deeper mineral horizons or aluminosilicate weathering (Bagard et al., 2011; Vasyukova et al., 2019), and possibly with release from reactive suspended particulate matter (Krickov et al., 2020; Lim et al., 2024). Al shows negative relationships with labile cations and anions (DIC, Ca, Mg, P, As), indicating contrasting source domains and transport pathways between mineral-groundwater-derived solutes and colloid-associated lithogenic elements.

Colloids exert strong control on trace-element export due to their dual organic–mineral character. Organic ligands of predominantly fulvic composition efficiently complex divalent transition metals, whereas association of trivalent and tetravalent hydrolysates—including uranyl species—with Fe and Al oxyhydroxides stabilized by organic polymers represent highly effective pathways for enhancing the apparent mobility of otherwise insoluble lithogenic elements (Vasyukova et al., 2010; Krickov et al., 2019, 2025). Importantly, the colloidal organization observed in the Low Lena—entirely located within the continuous permafrost zone—does not differ substantially from patterns reported for the Ob River (Kolesnichenko et al., 2021), western Siberian rivers spanning a permafrost gradient (Krickov et al., 2019), the permafrost-free Severnaya Dvina (Pokrovsky et al., 2010), or boreal rivers of northwestern European Russia (Ilina et al., 2016; Vasyukova et al., 2010). The proportion of colloidal forms of individual major and trace solutes within the three principal geochemical groups identified here varies

https://doi.org/10.5194/egusphere-2026-2540
Preprint. Discussion started: 13 May 2026

by less than ±20% relative to these systems. This convergence suggests that permafrost presence alone does not fundamentally alter the colloidal transport architecture of large boreal and Arctic rivers during summer baseflow, despite its strong influence on hydrological routing and active-layer dynamics. A similar conclusion was reached in earlier studies of Fe-rich colloids in the Lena basin (Hirst et al., 2017).

4.2.3. Multivariate confirmation of transport structure

PCA results corroborate pairwise correlations and confirm the dual (colloidal versus dissolved) control on solute export. The first factor separates lithogenic, low-solubility elements (Al and associated trivalent/tetravalent trace elements) from highly soluble weathering-derived constituents (B, SO_4, DIC, Mg, Sr), reflecting the contrast between colloidal transport and groundwater connectivity. The second factor captures latitudinal variability in DOC and labile nutrients, highlighting the surface-derived contribution to solute patterns. Similar factorial structures have been reported in rivers across western Siberia (Kolesnichenko et al., 2021; Pokrovsky et al., 2016a, 2020, 2022a, b; Krickov et al., 2019, 2025, 2026; Vorobyev et al., 2024) and in the upper and middle Lena during spring flood (Vorobyev et al., 2021b), indicating persistent large-scale controls on Arctic river solute organization across hydrological seasons. Taken together, the agreement with long-term monitoring data and independent spatial surveys, combined with size-fractionation and multivariate analyses, demonstrates that major solute export in the Low Lena is buffered and groundwater-dominated, whereas trace-element mobility is largely governed by stable organic and organo-mineral colloidal carriers, yielding a transport structure that is remarkably consistent with other Arctic and boreal river systems.

Importantly, the dominance of stable organic–mineral colloidal carriers provides a mechanistic explanation for the apparent decoupling between bulk dissolved carbon pools and CO_2 supersaturation observed along the Low Lena main stem. While DOC and associated trace elements are largely transported within organic supramolecular and organo-mineral colloids that buffer their concentrations over long distances, CO_2 reflects the instantaneous balance between lateral supply, in-stream respiration, and hydrodynamic evasion. In other words, the colloidal matrix stabilizes carbon and trace-element stocks within the rather inert dissolved pool, whereas gaseous CO_2 responds rapidly to metabolic and

https://doi.org/10.5194/egusphere-2026-2540
Preprint. Discussion started: 13 May 2026

physical processing at very short temporal and spatial scale. This functional separation between structurally buffered dissolved carbon and dynamically regulated CO_2 supersaturation may be a characteristic feature of large Arctic rivers, where extensive basin integration and colloidal transport dampen longitudinal variability in bulk solutes despite active atmospheric carbon exchange.

5. Conclusions

Large Arctic rivers are key regulators of lateral carbon transfer and atmospheric carbon exchange. By combining continuous in situ pCO_2 measurements, chamber-based fluxes, multivariate statistics, and size-fractionation analyses along ~800 km of the Low Lena main stem and its major tributaries, this study provides an integrated view of carbon dynamics and solute transport in one of the world's largest permafrost-dominated river systems.

During the post-freshet recession, CO_2 concentrations and emissions showed strong local variability but no systematic south–north gradient. Fluxes were comparable to those reported for the middle Lena, the Low Ob, and other large Siberian rivers, confirming the Lena as a moderate but persistent CO_2 source during the open-water season. The highest emissions occurred in the Vilyui tributary, underlining the role of large sub-basins in regulating main-stem carbon evasion. In contrast, DOC and DIC remained relatively stable along the transect, highlighting a functional decoupling between dissolved carbon pools and gaseous CO_2 dynamics.

Size-fractionation, correlation analysis, and PCA revealed a dual geochemical structure of dissolved solutes. Mobile major ions, Si, and oxyanion-forming trace elements were mainly present in truly dissolved form and reflected groundwater connectivity and interaction with soluble lithologies. By contrast, lithogenic low-solubility elements, especially trivalent and tetravalent hydrolysates, were transported predominantly in organo-mineral colloidal form and were associated with Al, Fe, and DOC, indicating mobilization via surface and suprapermafrost flow pathways.

This organization is consistent with patterns reported for other Arctic and boreal rivers, suggesting that colloidal buffering of refractory elements is a generic feature of organic-rich fluvial systems. Continuous permafrost does not fundamentally alter this summer transport architecture, but

https://doi.org/10.5194/egusphere-2026-2540
Preprint. Discussion started: 13 May 2026

mainly controls hydrological routing and exchange with deeper groundwater. Under ongoing Arctic warming, changes in discharge, vegetation, and surface-flow connectivity are therefore likely to affect Lena hydrochemistry more strongly than direct thermal effects, while winter talik development may exert stronger influence on labile solutes and inorganic carbon export.

Authors contribution: Y.Ya.K., V.A.N., O.V.D., D.V.C., E.A.S., A.V.K., V.A.K carried field work ; O.S.P, Y.Ya.K, S.N.V. performed the analyses; S.N.V and I.P.S. contributed to the interpretation of the results. Y.Ya.K., I.P.S and O.S.P took the lead in writing the manuscript. All authors provided critical feedback and helped shape the research, analysis and manuscript.

Data availability: All primary data are presented in the Supplementary Material

Acknowledgements:

Partial support from Priority-2030 Programme of the TSU is acknowledged. OP was partially supported by the project PEACE of PEPR FairCarboN ANR-22-PEXF-0011. IS and DCh were partially supported by the Russian Ministry of Science and High Education by the projects (FEFF-2024-0004, FEFF-2026-0007) to SakhGU.

References

Ahmed, R., Prowse, T., Dibike, Y., Bonsal, B., O'Neil, H.: Recent trends in freshwater influx to the Arctic Ocean from four major Arctic-draining rivers, Water 12, 1189, https://doi.org/10.3390/w12041189, 2020.

Alin, S.R., Rasera, M.F.F.L., Salimon, C.I., Richey, J.E., Holtgrieve, G.W., Krusche, A.V., et al.: Physical controls on carbon dioxide transfer velocity and flux in low-gradient river systems and implications for regional carbon budgets, J. Geophys. Res. Biogeosci. 116, G01009, https://doi.org/10.1029/2010JG001398, 2011.

Allen, G.H., Pavelsky, T.M.: Global extent of rivers and streams, Science 361, 585–588, https://doi.org/10.1126/science.aat0636, 2018.

Attermeyer, K., Catalan, N., Einarsdottir, K., Freixa, A., Groeneveld, M., Hawkes, J.A., et al.: Organic carbon processing during transport through boreal inland waters: particles as important sites, J. Geophys. Res. Biogeosci. 123, 2412–2428, https://doi.org/10.1029/2018JG004500, 2018.

Bagard, M.L., Chabaux, F., Pokrovsky, O.S., Viers, J., Prokushkin, A.S., Stille, P., Rihs, S., Schmitt, A.D., Dupré, B.: Seasonal variability of element fluxes in two Central Siberian rivers draining high latitude permafrost dominated areas, Geochim. Cosmochim. Acta 75, 3335–3357, 2011.

Beckebanze, L., Runkle, B.R.K., Walz, J., Wille, C., Holl, D., Helbig, M., Boike, J., Sachs, T., Kutzbach, L.: Lateral carbon export has low impact on the net ecosystem carbon balance of a

https://doi.org/10.5194/egusphere-2026-2540
Preprint. Discussion started: 13 May 2026

polygonal tundra catchment, Biogeosciences 19, 3863–3876, https://doi.org/10.5194/bg-19-3863-2022, 2022.
Berezovskaya, S., Yang, D., Hinzman, L.: Long-term annual water balance analysis of the Lena River, Glob. Planet. Change 48, 84–95, https://doi.org/10.1016/j.gloplacha.2004.12.006, 2005.
Brown, J., Ferrians Jr., O.J., Heginbottom, J.A., Melnikov, E.S.: Circum-Arctic map of permafrost and ground-ice conditions, National Snow and Ice Data Center/World Data Center for Glaciology, Boulder, CO, USA, digital media, 2002.
Bussmann, I.: Distribution of methane in the Lena Delta and Buor-Khaya Bay, Russia, Biogeosciences 10, 4641–4652, https://doi.org/10.5194/bg-10-4641-2013, 2013.
Cai, W.-J., Wang, Y.: The chemistry, fluxes, and sources of carbon dioxide in the estuarine waters of the Satilla and Altamaha Rivers, Georgia, Limnol. Oceanogr. 43, 657–668, https://doi.org/10.4319/lo.1998.43.4.0657, 1998.
Cauwet, G., Sidorov, I.: The biogeochemistry of Lena River: organic carbon and nutrients distribution, Mar. Chem. 53, 211–227, https://doi.org/10.1016/0304-4203(95)00090-9, 1996.
Chevychelov, A.P., Bosikov, N.P.: Natural conditions, In: Troeva, E.I., et al. (Eds.), The Far North. Springer, Netherlands, p. 123, https://link.springer.com/chapter/10.1007/978-90-481-3774-9_1, 2010.
Chupakov, A.V., Pokrovsky, O.S., Shirokova, L.S., Moreva, O.Y., Neverova, N.V., Chupakova, A.A., Kotova, A.I., Vorobyeva, T.Y.: High resolution multi-annual riverine fluxes of organic carbon, nutrient and trace element from the largest European Arctic river, Severnaya Dvina, Chem. Geol. 538, 119491, 2020.
Chupakov, A.V., Pokrovsky, O.S., Moreva, O.Y., Kotova, E., Vorobyeva, T.Y., Shirokova, L.S.: Export of organic carbon, nutrient and metals by the medium-size Pechora River to the Arctic Ocean, Chem. Geol. 632, 121524, https://doi.org/10.1016/j.chemgeo.2023.121524, 2023.
Cole, J.J., Prairie, Y.T., Caraco, N.F., McDowell, W.H., Tranvik, L.J., Striegl, R.G., et al.: Plumbing the global carbon cycle: integrating inland waters into the terrestrial carbon budget, Ecosystems 10, 171–184, 2007.
Cooper, L.W., McClelland, J.W., Holmes, R.M., Raymond, P.A., Gibson, J.J., Guay, C.K., Peterson, B.J.: Flow-weighted values of runoff tracers (δ18O, DOC, Ba, alkalinity) from the six largest Arctic rivers, Geophys. Res. Lett. 35, L18606, https://doi.org/10.1029/2008GL035007, 2008.
Crawford, J.T., Striegl, R.G., Wickland, K.P., Dornblaser, M.M., Stanley, E.H.: Emissions of carbon dioxide and methane from a headwater stream network of interior Alaska, J. Geophys. Res. Biogeosci. 118, 482–494, 2013.
Cuss, C.W., Grant-Weaver, I., Shotyk, W.: AF4-ICPMS with the 300 Da membrane to resolve metal-bearing 'colloids' <1 kDa: optimization, fractogram deconvolution, and advanced quality control, Anal. Chem. 89, 8027–8035, 2017.
Cuss, C.W., Donner, M.W., Grant-Weaver, I., Noernberg, T., Pelletier, R., Sinnatamby, R.N., Shotyk, W.: Measuring the distribution of trace elements amongst dissolved colloidal species as a fingerprint for contribution of tributaries to large boreal rivers, Sci. Total Environ. 642, 1242–1251, 2018.
Cuss, C.W., Glover, C.N., Javed, M.B., Nagel, A., Shotyk, W.: Geochemical and biological controls on the ecological relevance of total, dissolved, and colloidal forms of trace elements in large boreal rivers: review and case studies, Environ. Rev. 28, 138–163, https://doi.org/10.1139/er-2019-0014, 2020.
Dean, J.F., Meisel, O.H., Rosco, M.M., et al.: East Siberian Arctic inland waters emit mostly contemporary carbon, Nat. Commun. 11, 1627, https://doi.org/10.1038/s41467-020-15511-6, 2020.
Denfeld, B.A., Frey, K.E., Sobczak, W.V., Mann, P.J., Holmes, R.M.: Summer CO2 evasion from streams and rivers in the Kolyma River basin, north-east Siberia, Polar Res. 32, 19704, https://doi.org/10.3402/polar.v32i0.19704, 2013.
Drake, T.W., Raymond, P.A., Spencer, R.G.M.: Terrestrial carbon inputs to inland waters: a current synthesis of estimates and uncertainty, Limnol. Oceanogr. Lett. 3, 132–142, https://doi.org/10.1002/lol2.10055, 2018.

https://doi.org/10.5194/egusphere-2026-2540
Preprint. Discussion started: 13 May 2026

Dudarev, O.V., Semiletov, I.P., Charkin, A.N.: Particulate material composition in the Lena River-Laptev Sea system: scales of heterogeneities, Dokl. Earth Sci. 411A, 1445–1451, 2006.
Eckhardt, T., Knoblauch, C., Kutzbach, L., Holl, D., Simpson, G., Abakumov, E., Pfeiffer, E.-M.: Partitioning net ecosystem exchange of CO2 on the pedon scale in the Lena River Delta, Siberia, Biogeosciences 16, 1543–1562, https://doi.org/10.5194/bg-16-1543-2019, 2019.
Feng, X.J., Vonk, J.E., van Dongen, B.E., Gustafsson, Ö., Semiletov, I.P., Dudarev, O.V., Wang, Z.H., Montluçon, D.B., Wacker, L., Eglinton, T.I.: Differential mobilization of terrestrial carbon pools in Eurasian Arctic river basins, Proc. Natl. Acad. Sci. U.S.A. 110, 14168–14173, https://doi.org/10.1073/pnas.1307031110, 2013.
Franz, D., Larmanou, E., Bornemann, N., Langer, M., Boike, J., Sachs, T.: Exchange of CO2 and CH4 between a Siberian thaw lake and the atmosphere, In: Proceedings of the XI International Conference on Permafrost, Potsdam, 20–24 June 2016, 2016.
Frey, K.E., Smith, L.C.: Amplified carbon release from vast West Siberian peatlands by 2100, Geophys. Res. Lett. 32, L09401, https://doi.org/10.1029/2004GL022025, 2005.
Frey, K.E., Siegel, D.I., Smith, L.C.: Geochemistry of West Siberian streams and their potential response to permafrost degradation, Water Resour. Res. 43, W03406, https://doi.org/10.1029/2006WR004902, 2007.
Gautier, E., Depret, T., Costard, F., Virmoux, C., Fedorov, A., et al.: Going with the flow: hydrologic response of middle Lena River (Siberia) to climate variability and change, J. Hydrol. 557, 475–488, https://doi.org/10.1016/j.jhydrol.2017.12.034, 2018.
Gebhardt, A.C., Gaye-Haake, B., Unger, D., Lahajnar, N., Ittekkot, V.: A contemporary sediment and organic carbon budget for the Kara Sea shelf (Siberia), Mar. Geol. 220, 83–100, https://doi.org/10.1016/j.margeo.2005.06.035, 2005.
Gelfan, A., Gustafsson, D., Motovilov, Y., Arheimer, B., Kalugin, A., Krylenko, I., Lavrenov, A.: Climate change impact on the water regime of two great Arctic rivers: modelling and uncertainty issues, Clim. Change 414, 499–515, https://doi.org/10.1007/s10584-016-1710-5, 2017.
Georgiadi, A.G., Tananaev, N.I., Dukhova, L.A.: Hydrochemical conditions at the Lena River in August 2018, Oceanology 59, 797–800, https://doi.org/10.1134/S0001437019050072, 2019.
Gonçalves-Araujo, R., Stedmon, C.A., Heim, B., Dubinenkov, I., Kraberg, A., Moiseev, D., Bracher, A.: From fresh to marine waters: characterization and fate of dissolved organic matter in the Lena River delta region, Siberia, Front. Mar. Sci. 2, 108, https://doi.org/10.3389/fmars.2015.00108, 2015.
Gordeev, V.V., Sidorov, I.S.: Concentrations of major elements and their outflow into the Laptev Sea by the Lena River, Mar. Chem. 43, 33–46, 1993.
Gordeev, V.V., Martin, J.-M., Sidorov, I.S., Sidorova, M.V.: A reassessment of the Eurasian river input of water, sediment, major elements, and nutrients to the Arctic Ocean, Am. J. Sci. 296, 664–691, 1996.
Gordeev, V.V., Rachold, V., Vlasova, I.E.: Geochemical behavior of major and trace elements in suspended particulate material of the Irtysh River, the main tributary of the Ob River, Siberia, Appl. Geochem. 19, 593–610, 2004.
Gordeev, V.V., Pokrovsky, O.S., Zhulidov, A.V., Filippov, A.S., Gurtovaya, T.Y., Holmes, R.M., Kosmenko, L.S., McClelland, J.W., Peterson, B.J., Tank, S.E.: Dissolved major and trace elements in the largest Eurasian Arctic rivers: Ob, Yenisey, Lena, and Kolyma, Water 16, 316, https://doi.org/10.3390/w16020316, 2024.
Griffin, C.G., McClelland, J.W., Frey, K.E., Fiske, G., Holmes, R.M.: Quantifying CDOM and DOC in major Arctic rivers during ice-free conditions using Landsat TM and ETM+ data, Remote Sens. Environ. 209, 395–409, https://doi.org/10.1016/j.rse.2018.02.060, 2018.
Guérin, F., Abril, G., Serça, D., Delon, C., Richard, S., Delmas, R., Tremblay, A., Varfalvy, L.: Gas transfer velocities of CO2 and CH4 in a tropical reservoir and its river downstream, J. Mar. Syst. 66, 161–172, https://doi.org/10.1016/j.jmarsys.2006.03.019, 2007.
Hirst, C., Andersson, P.S., Shaw, S., Burke, I.T., Kutscher, L., Murphy, M.J., Maximov, T., Pokrovsky, O.S., Mörth, C.-M., Porcelli, D.: Characterisation of Fe-bearing particles and colloids in the Lena

https://doi.org/10.5194/egusphere-2026-2540
Preprint. Discussion started: 13 May 2026

River basin, NE Russia, Geochim. Cosmochim. Acta 213, 553–573, https://doi.org/10.1016/j.gca.2017.07.012, 2017.

Hirst, K., Andersson, P., Kooijman, E., Kutscher, L., Maximov, T., Mörth, C.-M., Porcelli, D.: Iron isotopes reveal the sources of Fe-bearing particles and colloids in the Lena River basin, Geochim. Cosmochim. Acta 269, 678–692, https://doi.org/10.1016/j.gca.2019.11.004, 2020.

Holmes, R.M., Peterson, B.J., Gordeev, V.V., Zhulidov, A.V., Meybeck, M., Lammers, R.B., Vörösmarty, C.J.: Flux of nutrients from Russian rivers to the Arctic Ocean: can we establish a baseline against which to judge future changes? Water Resour, Res. 36, 2309–2320, 2000.

Holmes, R.M., Peterson, B.J., Zhulidov, A.V., Gordeev, V.V., Makkaveev, P.N., Stunzhas, P.A., Kosmenko, L.S., Köhler, G.H., Shiklomanov, A.I.: Nutrient chemistry of the Ob' and Yenisey Rivers, Siberia: results from June 2000 expedition and evaluation of long-term data sets, Mar. Chem. 75, 219–227, 2001.

Holmes, R.M., Coe, M.T., Fiske, G.J., Gurtovaya, T., McClelland, J.W., Shiklomanov, A.I., Spencer, R.G.M., Tank, S.E., Zhulidov, A.V.: Climate change impacts on the hydrology and biogeochemistry of Arctic rivers, In: Goldman, C.R., Kumagai, M., Robarts, R.D. (Eds.), Climatic Changes and Global Warming of Inland Waters: Impacts and Mitigation for Ecosystems and Societies. John Wiley & Sons, pp. 1–26, 2013.

Hopkinson, C.S.: Shallow-water benthic and pelagic metabolism, Mar. Biol. 87, 19–32, https://doi.org/10.1007/BF00397002, 1985.

Horan, K., Hilton, R.G., Dellinger, M., Tipper, E., Galy, V., Calmels, D., Selby, D., Gaillardet, J., Ottley, C.J., Parsons, D.R., Burton, K.W.: Carbon dioxide emissions by rock organic carbon oxidation and the net geochemical carbon budget of the Mackenzie River Basin, Am. J. Sci. 319, 473–499, https://doi.org/10.2475/06.2019.02, 2019.

Hotchkiss, E., Hall Jr., R., Sponseller, R., et al.: Sources of and processes controlling CO2 emissions change with the size of streams and rivers, Nat. Geosci. 8, 696–699, https://doi.org/10.1038/ngeo2507, 2015.

Huh, Y., Tsoi, M.Y., Zaitsev, A., Edmond, J.M.: The fluvial geochemistry of the rivers of eastern Siberia: I, Tributaries of the Lena River draining the sedimentary platform of the Siberian Craton. Geochim. Cosmochim. Acta 62, 1657–1676, https://doi.org/10.1016/S0016-7037(98)00107-0, 1998a.

Huh, Y., Panteleyev, G., Babich, O., Zaitsev, A., Edmond, J.M.: The fluvial geochemistry of the rivers of Eastern Siberia: II, Tributaries of the Lena, Omoloy, Yana, Indigirka, Kolyma, and Anadyr draining the collisional/accretionary zone of the Verkhoyansk and Cherskiy ranges. Geochim. Cosmochim. Acta 62, 5063–5075, 1998b.

Huh, Y., Edmond, J.M.: The fluvial geochemistry of the rivers of Eastern Siberia: III, Tributaries of the Lena and Anabar draining the basement terrain of the Siberian Craton and the Trans-Baikal Highlands. Geochim. Cosmochim. Acta 63, 967–987, https://doi.org/10.1016/S0016-7037(99)00045-9, 1999.

Humborg, C., Mörth, C.-M., Sundbom, M., Borg, H., Blenckner, T., Giesler, R., Ittekkot, V.: CO2 supersaturation along the aquatic conduit in Swedish watersheds as constrained by terrestrial respiration, aquatic respiration and weathering, Glob. Change Biol. 16, 1966–1978, https://doi.org/10.1111/j.1365-2486.2009.02092.x, 2010.

Ilina, S.M., Lapitsky, S.A., Alekhin, Y.V., Viers, J., Benedetti, M., Pokrovsky, O.S.: Speciation, size fractionation and transport of trace element in the continuum soil water–mire–lake–river–large oligotrophic lake of a subarctic watershed, Aquat. Geochem. 22, 65–95, 2016.

Jähne, B., Heinz, G., Dietrich, W.: Measurement of the diffusion coefficients of sparingly soluble gases in water, J. Geophys. Res. Oceans 92, 10767–10776, https://doi.org/10.1029/JC092iC10p10767, 1987.

Johnson, M.S., Billett, M.F., Dinsmore, K.J., Wallin, M., Dyson, K.E., Jassal, R.S.: Direct and continuous measurement of dissolved carbon dioxide in freshwater aquatic systems: method and applications, Ecohydrology 3, 68–78, https://doi.org/10.1002/eco, 2009.

https://doi.org/10.5194/egusphere-2026-2540
Preprint. Discussion started: 13 May 2026

Juhls, B., Stedmon, C.A., Morgenstern, A., Meyer, H., Hölemann, J., Heim, B., Povazhnyi, V., Overduin, P.P.: Identifying drivers of seasonality in Lena River biogeochemistry and dissolved organic matter fluxes, Front. Environ. Sci. 8, 53, https://doi.org/10.3389/fenvs.2020.00053, 2020.

Juhls, B., Morgenstern, A., Hölemann, J., Eulenburg, A., Heim, B., Miesner, F., Grotheer, H., Mollenhauer, G., Meyer, H., Erkens, E., Gehde, F.Y., Antonova, S., Chalov, S., Tereshina, M., Erina, O., Fingert, E., Abramova, E., Sanders, T., Lebedeva, L., Torgovkin, N., Maksimov, G., Povazhnyi, V., Gonçalves-Araujo, R., Wünsch, U., Chetverova, A., Opfergelt, S., Overduin, P.P.: Lena River biogeochemistry captured by a 4.5-year high-frequency sampling program, Earth Syst. Sci. Data 17, 1–28, https://doi.org/10.5194/essd-17-1-2025, 2025.

Karlsson, J., Serikova, S., Rocher-Ros, G., Denfeld, B., Vorobyev, S.N., Pokrovsky, O.S.: Carbon emission from Western Siberian inland waters, Nat. Commun. 12, 825, https://doi.org/10.1038/s41467-021-21054-1, 2021.

Kipp, L.E., Henderson, P.B., Wang, Z.A., Charrette, M.A.: Deltaic and estuarine controls on Mackenzie River solute fluxes to the Arctic Ocean, Estuar. Coasts 43, 1992–2014, https://doi.org/10.1007/s12237-020-00739-8, 2020.

Kolesnichenko, I., Kolesnichenko, L.G., Vorobyev, S.N., Shirokova, L.S., Semiletov, I.P., Dudarev, O.V., Vorobev, R.S., Shavrina, U., Kirpotin, S.N., Pokrovsky, O.S.: Landscape, soil, lithology, climate and permafrost control on dissolved carbon, major and trace elements in the Ob River, Western Siberia, Water 13, 3189, https://doi.org/10.3390/w13223189, 2021.

Krickov, I.V., Pokrovsky, O.S., Manasypov, R.M., Lim, A.G., Shirokova, L.S., Viers, J.: Colloidal transport of carbon and metals by western Siberian rivers during different seasons across a permafrost gradient, Geochim. Cosmochim. Acta 265, 221–241, https://doi.org/10.1016/j.gca.2019.08.041, 2019.

Krickov, I.V., Lim, A.G., Manasypov, R.M., Loiko, S.V., Vorobyev, S.N., Shevchenko, V.P., Dara, O.M., Gordeev, V.V., Pokrovsky, O.S.: Major and trace elements in suspended matter of western Siberian rivers: first assessment across permafrost zones and landscape parameters of watersheds, Geochim. Cosmochim. Acta 269, 429–450, https://doi.org/10.1016/j.gca.2019.11.005, 2020.

Krickov, I.V., Lim, A.G., Korets, M., Shirokova, L.S., Karlsson, J., Pokrovsky, O.S.: Environmental controllers for carbon emission and concentration patterns in Siberian rivers during different seasons, Sci. Total Environ. 859, 160202, https://doi.org/10.1016/j.scitotenv.2022.160202, 2023.

Krickov, I.V., Vorobyev, S.N., Kolesnichenko, L.G., Kolesnichenko, Y., Zinchenko, D., Shirokova, L.S., Pokrovsky, O.S.: Export fluxes of dissolved, colloidal and particulate organic carbon, major and trace elements from the Ob River and its tributaries across seasons, Water Res. 275, 123221, https://doi.org/10.1016/j.watres.2025.123221, 2025.

Krickov, I.V., Loiko, S.V., Lim, A., Kuzmina, D.M., Istigechev, G.I., Shirokova, L.S., Pupyshev, Y.S., Pokrovsky, O.S.: Hydrological continuums across climate and permafrost gradients: spatial patterns of organic carbon, greenhouse gases, and major and trace elements, Water Res. 294, 125507, https://doi.org/10.1016/j.watres.2026.125507, 2026.

Kruse, S., Gerdes, A., Kath, N.J., Epp, L.S., Stoof-Leichsenring, K.R., Pestryakova, L.A., Herzschuh, U.: Dispersal distances and migration rates at the arctic treeline in Siberia – a genetic and simulation-based study, Biogeosciences 16, 1211–1224, https://doi.org/10.5194/bg-16-1211-2019, 2019.

Kutscher, L., Mörth, C.-M., Porcelli, D., Hirst, C., Maximov, T.C., Petrov, R.E., Andersson, P.S.: Spatial variation in concentration and sources of organic carbon in the Lena River, Siberia, J. Geophys. Res. Biogeosci. 122, 1999–2014, https://doi.org/10.1002/2017JG003858, 2017.

Kutzbach, L., Wille, C., Pfeiffer, E.-M.: The exchange of carbon dioxide between wet arctic tundra and the atmosphere at the Lena River Delta, Northern Siberia, Biogeosciences 4, 869–890, https://doi.org/10.5194/bg-4-869-2007, 2007.

Kuzmin, M.I., Tarasova, E.N., Bychinskii, V.A., Karabanov, E.B., Mamontov, A.A., Mamontova, E.A.: Hydrochemical regime components of Lena water, Water Resour. 36, 418–430, https://doi.org/10.1134/S0097807809040058, 2009.

https://doi.org/10.5194/egusphere-2026-2540
Preprint. Discussion started: 13 May 2026

Lara, R.J., Rachold, V., Kattner, G., Hubberten, H.-W., Guggenberger, G., Annelie, S., Thomas, D.N.: Dissolved organic matter and nutrients in the Lena River, Siberian Arctic: characteristics and distribution, Mar. Chem. 59, 301–309, https://doi.org/10.1016/S0304-4203(97)00076-5, 1998.

Lauerwald, R., Laruelle, G.G., Hartmann, J., Ciais, P., Regnier, P.A.G.: Spatial patterns in CO2 evasion from the global river network, Global Biogeochem. Cycles 29, 534–554, https://doi.org/10.1002/2014GB004941, 2015.

Leith, F.I., Garnett, M.H., Dinsmore, K.J., Billett, M.F., Heal, K.V.: Source and age of dissolved and gaseous carbon in a peatland-riparian-stream continuum: a dual isotope (14C and δ13C) analysis, Biogeochemistry 119, 415–433, https://doi.org/10.1007/s10533-014-9977-y, 2014.

Leith, F.I., Dinsmore, K.J., Wallin, M.B., Billett, M.F., Heal, K.V., Laudon, H., Öquist, M.G., Bishop, K.: Carbon dioxide transport across the hillslope–riparian–stream continuum in a boreal headwater catchment, Biogeosciences 12, 1–12, https://doi.org/10.5194/bg-12-1-2015, 2015.

Lim, A.G., Krickov, I.V., Vorobyev, S.N., Shirokova, L.S., Korets, M.A., Karlsson, J., Pokrovsky, O.S.: Carbon emission and export from the Ket River basin, western Siberia, Biogeosciences, 19, 5859–5877,, https://doi.org/10.5194/bg-19-1-2022, 2022.

Lim, A.G., Krickov, I.V., Pokrovsky, O.S.: Organic carbon, major and trace element release from and adsorption onto riverine particulate suspended matter: experimental approach, Sci. Total Environ. 948, 174735, https://doi.org/10.1016/j.scitotenv.2024.174735, 2024.

Lobbes, J.M., Fitznar, H.P., Kattner, G.: Biogeochemical characteristics of the dissolved and particulate organic matter in Russian rivers entering the Arctic Ocean, Geochim. Cosmochim. Acta 64, 2973–2983, 2000.

Loiko, S.V., Pokrovsky, O.S., Raudina, T.V., Lim, A., Kolesnichenko, L.G., Shirokova, L.S., Vorobyev, S.N., Kirpotin, S.N.: Abrupt permafrost collapse enhances organic carbon, CO2, nutrient and metal release into surface waters, Chem. Geol. 471, 153–165, 2017.

Marie, D., Partensky, F., Vaulot, D., Brussaard, C.: Enumeration of phytoplankton, bacteria, and viruses in marine samples, Curr. Protoc. Cytom. 10, 11111–111115, https://doi.org/10.1002/0471142956.cy1111s10, 1999.

Mavromatis, V.M., Porcelli, D., Andersson, P., Korets, M., Pokrovsky, O.S.: Lithological controls of the Mg isotope composition of the Lena River and its tributaries across seasons, Chem. Geol. 648, 121957, https://doi.org/10.1016/j.chemgeo.2024.121957, 2024.

McClelland, J.W., Holmes, R.M., Peterson, B.J., Strieglitz, M.: Increasing river discharge in the Eurasian Arctic: consideration of dams, permafrost thaw, and fires as potential agents of change, J. Geophys. Res. Atmos. 109, D18102, https://doi.org/10.1029/2004JD004583, 2004.

McClelland, J.W., Déry, S.J., Peterson, B.J., Holmes, R.M., Wood, E.F.: A pan-Arctic evaluation of changes in river discharge during the latter half of the 20th century, Geophys. Res. Lett. 33, L06715, https://doi.org/10.1029/2006GL025753, 2006.

Mu, C., Li, K., Liu, S., et al.: Recent intensified riverine CO2 emission across the Northern Hemisphere permafrost region, Nat. Commun. 16, 3616, https://doi.org/10.1038/s41467-025-58716-3, 2025.

Murphy, M., Porcelli, D., Pogge von Strandmann, P., Hirst, K., Kutscher, L., Katchinoff, J., Mörth, C.-M., Maximov, T., Andersson, P.: Tracing silicate weathering processes in the permafrost-dominated Lena River watershed using lithium isotopes, Geochim. Cosmochim. Acta 245, 154–171, https://doi.org/10.1016/j.gca.2018.10.024, 2018.

Ogneva, O., Mollenhauer, G., Juhls, B., Sanders, T., Palmtag, J., Fuchs, M., Grotheer, H., Mann, P.J., Strauss, J.: Particulate organic matter in the Lena River and its delta: from the permafrost catchment to the Arctic Ocean, Biogeosciences 20, 1423–1441, https://doi.org/10.5194/bg-20-1423-2023, 2023.

Pipko, I.I., Pugach, S.P., Savichev, O.G., Repina, I.A., Shakhova, N.E., Moiseeva, Yu.A., Barskov, K.V., Sergienko, V.I., Semiletov, I.P.: Dynamics of dissolved inorganic carbon and CO2 fluxes between the water and the atmosphere in the main channel of the Ob River, Dokl. Chem. 484, 52–57, https://doi.org/10.1134/S0012500819020101, 2019.

Pipko, I.I., Pugach, S.P., Dudarev, O.V., Charkin, A.N., Semiletov, I.P.: Carbonate parameters of the Lena River: characteristics and distribution, Geochem. Int. 48, 1131–1137, https://doi.org/10.1134/S0016702910110078, 2010.

https://doi.org/10.5194/egusphere-2026-2540
Preprint. Discussion started: 13 May 2026

Pokrovsky, O.S., Viers, J., Shirokova, L.S., Shevchenko, V.P., Filippov, A.S., Dupré, B.: Dissolved, suspended, and colloidal fluxes of organic carbon, major and trace elements in Severnaya Dvina River and its tributary, Chem. Geol. 273, 136–149, 2010.

Pokrovsky, O.S., Manasypov, R.M., Loiko, S.V., Shirokova, L.S.: Organic and organo-mineral colloids in discontinuous permafrost zone, Geochim. Cosmochim. Acta 188, 1–20, 2016a.

Pokrovsky, O.S., Manasypov, R.M., Loiko, S., Krickov, I.A., Kopysov, S.G., Kolesnichenko, L.G., Vorobyev, S.N., Kirpotin, S.N.: Trace element transport in western Siberia rivers across a permafrost gradient, Biogeosciences 13, 1877–1900, 2016b.

Pokrovsky, O.S., Lim, A.G., Krickov, I.V., Korets, M.A., Shirokova, L.S., Vorobyev, S.N.: Hydrochemistry of medium-size pristine rivers in boreal and subarctic zone: disentangling effect of landscape parameters across a permafrost, climate, and vegetation gradient, Water 14, 2250, https://doi.org/10.3390/w14142250, 2022a.

Pokrovsky, O.S., Manasypov, R.M., Chupakov, A.V., Kopysov, S.: Element transport in the Taz River, western Siberia, Chem. Geol. 614, 121180, https://doi.org/10.1016/j.chemgeo.2022.121180, 2022b.

Qin, J., Huh, Y., Edmond, J.M., Du, G., Ran, J.: Chemical and physical weathering in the Min Jiang, a headwater tributary of the Yangtze River, Chem. Geol. 227, 53–69, https://doi.org/10.1016/j.chemgeo.2005.09.011, 2006.

Rachold, V., Alabyan, A., Hubberten, H.-W., Korotaev, V.N., Zaitsev, A.A.: Sediment transport to the Laptev Sea: hydrology and geochemistry of the Lena River, Polar Res. 15, 183–196, https://doi.org/10.3402/polar.v15i2.6646, 1996.

Raudina, T.V., Loiko, S.V., Lim, A., Manasypov, R.M., Shirokova, L.S., Istigechev, G.I., Kuzmina, D.M., Kulizhsky, S.P., Vorobyev, S.N., Pokrovsky, O.S.: Permafrost thaw and climate warming may decrease the CO2, carbon, and metal concentration in peat soil waters of the Western Siberia Lowland, Sci. Total Environ. 634, 1004–1023, 2018.

Raudina, T.V., Loiko, S., Kuzmina, D.M., Shirokova, L.S., Kulizhsky, S.P., Golovatskaya, E.A., Pokrovsky, O.S.: Colloidal organic carbon and trace elements in peat porewaters across a permafrost gradient in Western Siberia, Geoderma 390, 114971, https://doi.org/10.1016/j.geoderma.2021.114971, 2021.

Raymond, P.A., Hartmann, J., Lauerwald, R., Sobek, S., McDonald, C., Hoover, M., Butman, D., Striegl, R., Mayorga, E., Humborg, C., Kortelainen, P., Dürr, H., Meybeck, M., Ciais, P., Guth, P.: Global carbon dioxide emissions from inland waters, Nature 503, 355–359, https://doi.org/10.1038/nature12760, 2013.

Rocher-Ros, G., Sponseller, R.A., Lidberg, W., Mörth, C.-M., Giesler, R.: Landscape process domains drive patterns of CO2 evasion from river networks, Limnol. Oceanogr. Lett. 4, 87–95, https://doi.org/10.1002/lol2.10108, 2019.

Rocher-Ros, G., Stanley, E.H., Loken, L.C., et al.: Global methane emissions from rivers and streams, Nature 621, 530–535, https://doi.org/10.1038/s41586-023-06344-6, 2023.

Sachs, T., Wille, C., Boike, J., Kutzbach, L.: Environmental controls on ecosystem-scale CH4 emission from polygonal tundra in the Lena River Delta, Siberia, J. Geophys. Res. Biogeosci. 113, G00A03, https://doi.org/10.1029/2007JG000505, 2008.

Savenko, A.V., Savenko, V.S.: Trace element composition of the dissolved matter runoff of the Russian Arctic rivers, Water 16, 565, https://doi.org/10.3390/w16040565, 2024.

Schuur, E.A.G., McGuire, A.D., Schädel, C., Grosse, G., Harden, J.W., Hayes, D.J., Hugelius, G., Koven, C.D., Kuhry, P., Lawrence, D.M., Natali, S.M., Olefeldt, C., Romanovsky, V.E., Schaefer, K., Turetsky, M.R., Treat, C.C., Vonk, J.E.: Climate change and the permafrost carbon feedback, Nature 520, 171–179, https://doi.org/10.1038/nature14338, 2015.

Semiletov, I.P.: Aquatic sources and sinks of CO2 and CH4 in the polar regions, J. Atmos. Sci. 56, 286–306, https://doi.org/10.1175/1520-0469(1999)056<0286:ASASOC>2.0.CO;2, 1999.

Semiletov, I.P., Pipko, I.I., Shakhova, N.E., Dudarev, O.V., Pugach, S.P., Charkin, A.N., McRoy, C.P., Kosmach, D., Gustafsson, Ö.: Carbon transport by the Lena River from its headwaters to the Arctic Ocean, with emphasis on fluvial input of terrestrial particulate organic carbon vs, carbon transport by coastal erosion. Biogeosciences 8, 2407–2426, https://doi.org/10.5194/bg-8-2407-2011, 2011.

https://doi.org/10.5194/egusphere-2026-2540
Preprint. Discussion started: 13 May 2026

Serikova, S., Pokrovsky, O.S., Ala-aho, P., Kazantsev, V., Kirpotin, S.N., Kopysov, S.G., Krickov, I.V., Laudon, H., Manasypov, R.M., Shirokova, L.S., Soulsby, C., Tetzlaff, D., Karlsson, J.: High riverine CO2 emissions at the permafrost boundary of Western Siberia, Nat. Geosci. 11, 825–829, https://doi.org/10.1038/s41561-018-0218-1, 2018.

Serikova, S., Pokrovsky, O.S., Laudon, H., Krickov, I.V., Lim, A.G., Manasypov, R.M., Karlsson, J.: C emissions from lakes across permafrost gradient of Western Siberia, Nat. Commun. 10, 1552, https://doi.org/10.1038/s41467-019-09592-1, 2019.

Siewert, M.B., Hugelius, G., Heim, B., Faucherre, S.: Landscape controls and vertical variability of soil organic carbon storage in permafrost-affected soils of the Lena River Delta, Catena 147, 725–741, https://doi.org/10.1016/j.catena.2016.07.048, 2016.

Smith, L.C., Pavelsky, T.M.: Estimation of river discharge, propagation speed, and hydraulic geometry from space: Lena River, Siberia, Water Resour. Res. 44, W03427, https://doi.org/10.1029/2007WR006133, 2008.

Spence, J., Telmer, K.: The role of sulfur in chemical weathering and atmospheric CO2 fluxes: evidence from major ions, δ13CDIC, and δ34SSO4 in rivers of the Canadian Cordillera, Geochim. Cosmochim. Acta 69, 5441–5458, https://doi.org/10.1016/j.gca.2005.07.011, 2005.

Stolpe, B., Guo, L., Shiller, A.: Binding and transport of rare earth elements by organic and iron-rich nanocolloids in Alaskan rivers, as revealed by field-flow fractionation and ICP-MS, Geochim. Cosmochim. Acta 106, 446–462, 2013a.

Stolpe, B., Guo, L., Shiller, A.M., Aiken, G.R.: Abundance, size distributions and trace-element binding of organic and iron-rich nanocolloids in Alaskan rivers, as revealed by field-flow fractionation and ICP-MS, Geochim. Cosmochim. Acta 105, 221–239, 2013b.

Striegl, R.G., Dornblaser, M.M., McDonald, C.P., Rover, J.R., Stets, E.G.: Carbon dioxide and methane emissions from the Yukon River system, Global Biogeochem. Cycles 26, GB0E05, https://doi.org/10.1029/2012GB004306, 2012.

Sun, X., Mörth, C.-M., Porcelli, D., Kutscher, L., Hirst, C., Murphy, M.J., Maximov, T., Petrov, R.E., Humborg, C., Schmitt, M., Andersson, P.S.: Stable silicon isotopic compositions of the Lena River and its tributaries: implications for silicon delivery to the Arctic Ocean, Geochim. Cosmochim. Acta 241, 120–133, https://doi.org/10.1016/j.gca.2018.08.044, 2018.

Suzuki, K., Matsuo, K., Yamazaki, D., Ichii, K., Iijima, Y., Papa, F., Yanagi, Y., Hiyama, T.: Hydrological variability and changes in the Arctic circumpolar tundra and the three largest Pan-Arctic river basins from 2002 to 2016, Remote Sens. 10, 402, https://doi.org/10.3390/rs10030402, 2018.

Tananaev, N., Lotsari, E.: Defrosting northern catchments: fluvial effects of permafrost degradation, Earth-Sci. Rev. 228, 103996, https://doi.org/10.1016/j.earscirev.2022.103996, 2022.

Tananaev, N.I., Makarieva, O.M., Lebedeva, L.S.: Trends in annual and extreme flows in the Lena River basin, Northern Eurasia, Geophys. Res. Lett. 43, 10764–10772, https://doi.org/10.1002/2016GL070796, 2016.

Tank, S.E., Raymond, P.A., Striegl, R.G., McClelland, J.W., Holmes, R.M., Fiske, G.J., Peterson, B.J.: A land-to-ocean perspective on the magnitude, source and implication of DIC flux from major Arctic rivers to the Arctic Ocean, Global Biogeochem. Cycles 26, GB4018, 2012.

Tank, S.E., McClelland, J.W., Spencer, R.G.M., Shiklomanov, A.I., Suslova, A., Moatar, F., Amon, R.M.W., Cooper, L.W., Elias, G., Gordeev, V.V., Guay, C., Gurtovaya, T.Y., Kosmenko, L.S., Mutter, E.A., Peterson, B.J., Peucker-Ehrenbrink, B., Raymond, P.A., Schuster, P.F., Scott, L., Staples, R., Striegl, R.G., Tretiakov, M., Zhulidov, A.V., Zimov, N., Zimov, S., Holmes, R.M.: Recent trends in the chemistry of major northern rivers signal widespread Arctic change, Nat. Geosci. 16, 789–796, https://doi.org/10.1038/s41561-023-01247-7, 2023.

Vachon, D., Prairie, Y.T., Cole, J.J.: The relationship between near-surface turbulence and gas transfer velocity in freshwater systems and its implications for floating chamber measurements of gas exchange, Limnol. Oceanogr. 55, 1723–1732, https://doi.org/10.4319/lo.2010.55.4.1723, 2010.

Vasyukova, E.V., Pokrovsky, O.S., Viers, J., Oliva, P., Dupré, B., Martin, F., Candaudap, F.: Trace elements in organic- and iron-rich surficial fluids of the boreal zone: assessing colloidal forms via dialysis and ultrafiltration, Geochim. Cosmochim. Acta 74, 449–468, 2010.

https://doi.org/10.5194/egusphere-2026-2540
Preprint. Discussion started: 13 May 2026

Vasyukova, E.V., Oliva, P., Viers, J., Martin, F., Dupré, B., Pokrovsky, O.S.: Chemical weathering of mafic rocks in boreal subarctic environment (North-West Russia) under influence of glacial moraine deposits, Chem. Geol. 509, 115–133, 2019.

Vonk, J.E., Tank, S.E., Mann, P.J., Spencer, R.G.M., Treat, C.C., Striegl, R.G., Abbott, B.W., Wickland, K.P.: Biodegradability of dissolved organic carbon in permafrost soils and aquatic systems: a meta-analysis, Biogeosciences 12, 6915–6930, https://doi.org/10.5194/bg-12-6915-2015, 2015.

Vonk, J.E., Tank, S.E., Walvoord, M.A.: Integrating hydrology and biogeochemistry across frozen landscapes, Nat. Commun. 10, 1–4, https://doi.org/10.1038/s41467-019-13361-5, 2019.

Vonk, J., Speetjens, N.J., Poste, A.: Small watersheds may play a disproportionate role in Arctic land-ocean fluxes, Nat. Commun. 14, https://doi.org/10.1038/s41467-023-39209-7, 2023.

Vorobyev, S.N., Pokrovsky, O.S., Kolesnichenko, L.G., Manasypov, R.M., Shirokova, L.S., Karlsson, J., Kirpotin, S.N.: Biogeochemistry of dissolved carbon, major, and trace elements during spring flood periods on the Ob River, Hydrol. Process. 33, 1579–1594, https://doi.org/10.1002/hyp.13424, 2019.

Vorobyev, S.N., Karlsson, J., Kolesnichenko, Y.Y., Korets, M., Pokrovsky, O.S.: Fluvial carbon dioxide emission from the Lena River basin during the spring flood, Biogeosciences 18, 4919–4936, https://doi.org/10.5194/bg-18-4919-2021, 2021a.

Vorobyev, S.N., Kolesnichenko, Y., Korets, M., Pokrovsky, O.S.: Testing landscape, climate and lithology impact on hydrochemical features of the Lena River and its tributaries, Water (MDPI) 13, Art No 2093, https://doi.org/10.3390/w13152093, 2021b.

Vorobyev, S.N., Kolesnichenko, Y., Karlsson, J., Pokrovsky, O.S.: Carbon emission from the Lower Ob River floodplain during spring flood, Sci. Total Environ. 954, 176294, https://doi.org/10.1016/j.scitotenv.2024.176294, 2024.

Wanninkhof, R.: Relationship between wind speed and gas exchange over the ocean, J. Geophys. Res. 97, 7373–7382, 1992.

Ward, C.P., Nalven, S.G., Crump, B.C., Kling, G.W., Cory, R.M.: Photochemical alteration of organic carbon draining permafrost soils shifts microbial metabolic pathways and stimulates respiration, Nat. Commun. 8, 772, https://doi.org/10.1038/s41467-017-00759-2, 2017.

Wegner, R., Fiencke, C., Knoblauch, C., Sauerland, L., Beer, C.: Rapid permafrost thaw removes nitrogen limitation rising the potential of N2O emissions, EGU General Assembly 2022, Vienna, Austria, 23–27 May 2022, EGU22-11181, https://doi.org/10.5194/egusphere-egu22-11181, 2022.

Wild, B., Andersson, A., Bröder, L., Vonk, J., Hugelius, G., McClelland, J.W., Song, W., Raymond, P.A., Gustafsson, Ö.: Rivers across the Siberian Arctic unearth the patterns of carbon release from the thawing permafrost, Proc. Natl. Acad. Sci. U.S.A. 116, 10280–10285, https://doi.org/10.1073/pnas.1811797116, 2019.

Wu, L., Huh, Y.: Dissolved reactive phosphorus in large rivers of East Asia, Biogeochemistry 85, 263–288, https://doi.org/10.1007/s10533-007-9133-z, 2007.

Yang, D.Q., Kane, D.L., Hinzman, L.D., Zhang, X.B., Zhang, T.J., Ye, H.C.: Siberian Lena River hydrological regime and recent change, J. Geophys. Res. Atmos. 107, 4694, https://doi.org/10.1029/2002JD002542, 2002.

Yamamoto, S., Alcauskas, J.B., Crozier, T.E.: Solubility of methane in distilled water and seawater, J. Chem. Eng. Data 21, 78–80, https://doi.org/10.1021/je60068a029, 1976.

Ye, B., Yang, D., Zhang, Z., Kane, D.L.: Variation of hydrological regime with permafrost coverage over Lena basin in Siberia, J. Geophys. Res. 114, D07102, https://doi.org/10.1029/2008JD010537, 2009.

Yeghicheyan, D., Aubert, D., Bouhnik-Le Coz, M., Chmeleff, J., Delpoux, S., Djouraev, I., Granier, G., Lacan, F., Piro, J.-L., Rousseau, T., Cloquet, C., Marquet, A., Menniti, C., Pradoux, C., Freydier, R., Vieira da Silva-Filho, E., Suchorski, K.: A new interlaboratory characterisation of silicon, rare earth elements and twenty-two other trace element concentrations in the natural river water certified reference material SLRS-6 (NRC-CNRC), Geostand. Geoanal. Res. 43, 475–496, https://doi.org/10.1111/ggr.12268, 2019.

https://doi.org/10.5194/egusphere-2026-2540
Preprint. Discussion started: 13 May 2026

Yoon, T.K., Jin, H., Oh, N.-H., Park, J.-H.: Technical note: assessing gas equilibration systems for continuous pCO2 measurements in inland waters, Biogeosciences 13, 3915–3930, https://doi.org/10.5194/bg-13-3915-2016, 2016.

Zhang, T., Frauenfeld, O.W., Serreze, M.C., Etringer, A., Oelke, C., et al.: Spatial and temporal variability in active layer thickness over the Russian Arctic drainage basin, J. Geophys. Res. 110, D16101, https://doi.org/10.1029/2004JD005642, 2005.

https://doi.org/10.5194/egusphere-2026-2540
Preprint. Discussion started: 13 May 2026

Table 1. Hydrochemical parameters of the Lena River main stem averaged across the entire transect from Yakutsk to Kyusur. Elemental concentrations (Li to U) are in µg/L.

Parameter	N	Mean	Std.Dev.	Median	Minimum	Maximum
pH	19	7.19	0.19	7.18	6.78	7.70
T_{water}, °C	26	17.56	1.32	17.60	15.30	20.20
O_2, mg/L	26	9.25	0.35	9.19	8.61	9.92
CO2, µatm	26	1019	419	892	609	2646
FCO_2, g C m^{-2} d^{-1}	11	0.29	0.17	0.25	0.11	0.68
CH_4, µmol/L	26	0.22	0.44	0.08	0.02	2.20
E.C., µS/cm	26	114	13	115	82	145
DIC, mg/L	26	8.42	2.66	8.47	4.07	18.45
DOC, mg/L	26	7.54	2.74	7.19	5.47	20.30
F-, mg/L	26	0.0665	0.02	0.07	0.03	0.12
Cl-, mg/L	26	3.52	2.13	3.41	0.60	9.71
Br-, mg/L	26	0.0028	0.00	0.00	0.00	0.00
N-NO_3-, mg/L	26	0.0155	0.01	0.01	0.00	0.03
S-SO_4^{2-}, mg/L	26	3.35	1.54	2.97	1.49	6.50
P-PO_4^{3-}, mg/L	18	0.0019	0.00	0.00	0.00	0.00
TBC, cells/mL	25	448680	383520	316930	59880	1341000
Li, µg/L	26	1.22	0.18	1.25	0.75	1.55
Be	26	0.0128	0.0029	0.0124	0.0086	0.022
B	26	9.58	2.81	8.63	3.30	17.4
Na	26	3411	1316	3580	1238	6526
Mg	26	2735	641	2706	1742	4120
Al	26	39.6	16.2	35.6	19.5	90.7
Si	26	1491	120	1501	1223	1780
P	26	5.55	2.09	4.9	3.1	10.8
K	26	530	238	432	338	1429
Ca	26	11160	4040	11040	6880	27380
Sc	26	0.0247	0.01	0.02	0.02	0.07
Ti	26	0.48	0.23	0.42	0.22	1.33
V	26	0.32	0.10	0.31	0.18	0.71
Cr	26	0.17	0.03	0.16	0.14	0.22
Mn	26	3.62	3.11	2.84	1.74	17.33
Fe	26	72.3	19.6	66.8	47.8	145
Co	26	0.056	0.03	0.05	0.03	0.15
Ni	26	0.54	0.29	0.45	0.33	1.76
Cu	26	1.30	0.78	0.95	0.73	4.50
Zn	26	70	160	25	4	835
Ga	26	0.03	0.01	0.03	0.02	0.08
As	26	0.16	0.05	0.17	0.09	0.34
Se	26	0.042	0.02	0.04	0.03	0.08
Rb	26	0.36	0.13	0.37	0.20	0.78
Sr	26	82.1	18.2	80.4	56.2	123.9
Y	26	0.17	0.05	0.17	0.10	0.34
Zr	26	0.12	0.08	0.11	0.06	0.51
Nb	26	0.0308	0.02	0.02	0.02	0.09
Mo	26	0.21	0.09	0.19	0.14	0.64

https://doi.org/10.5194/egusphere-2026-2540
Preprint. Discussion started: 13 May 2026

Cd	26	0.0199	0.02	0.01	0.01	0.10
Sn	25	0.33	1.12	0.04	0.00	5.52
Sb	26	0.029	0.01	0.03	0.01	0.07
Cs	26	0.0017	0.0007	0.0014	0.0008	0.0028
Ba	26	60.0	17.8	63.6	9.58	92
La	26	0.23	0.14	0.18	0.099	0.64
Ce	26	0.36	0.22	0.26	0.16	1.01
Pr	26	0.056	0.029	0.04	0.025	0.14
Nd	26	0.20	0.098	0.17	0.092	0.48
Sm	26	0.0435	0.016	0.04	0.022	0.086
Eu	26	0.0142	0.0025	0.01	0.010	0.019
Gd	26	0.0403	0.012	0.04	0.021	0.068
Tb	26	0.0055	0.0016	0.01	0.003	0.0089
Dy	26	0.0319	0.0093	0.03	0.017	0.055
Ho	26	0.0062	0.0018	0.01	0.0034	0.011
Er	26	0.0174	0.0052	0.02	0.0095	0.031
Tm	26	0.0024	0.0007	0.00	0.0014	0.0044
Yb	26	0.0162	0.0048	0.02	0.009	0.03
Lu	26	0.0024	0.0007	0.00	0.0013	0.0041
Hf	26	0.0890	0.049	0.08	0.049	0.31
W	26	0.0057	0.0025	0.01	0.0021	0.011
Tl	26	0.0015	0.0005	0.002	0.0007	0.003
Pb	26	0.090	0.038	0.08	0.05	0.19
Bi	26	0.0008	0.0002	0.00	0.0007	0.0013
Th	26	0.0309	0.024	0.02	0.0063	0.09
U	26	0.15	0.062	0.12	0.096	0.33

https://doi.org/10.5194/egusphere-2026-2540
Preprint. Discussion started: 13 May 2026

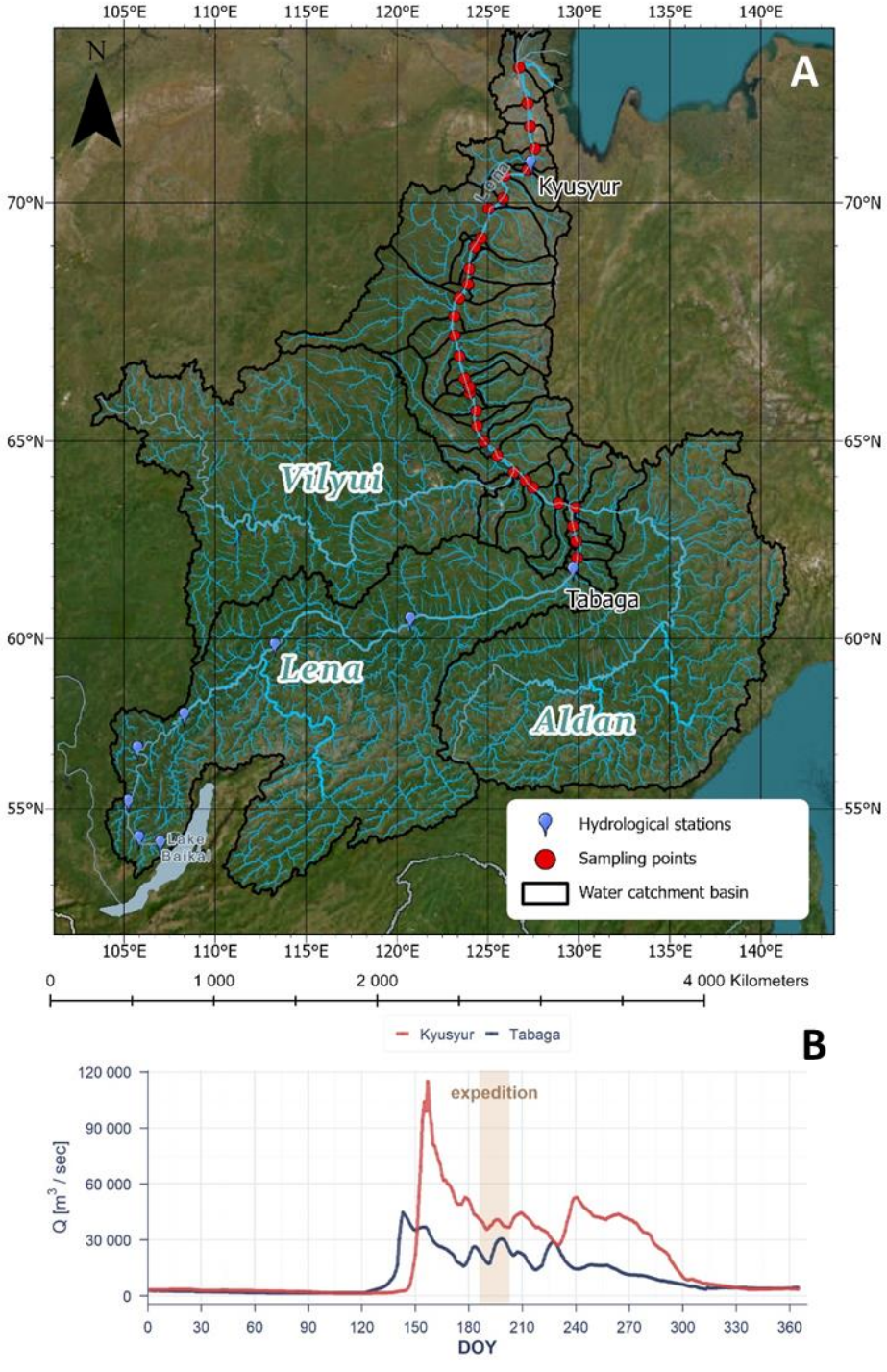

1218

1219 **Fig. 1. A**: The Lena River watershed and the position of sampling points of this study and **B**:
1220 Hydrograph of the Lena River in 2022 for the period of expedition (highlighted in pink).

https://doi.org/10.5194/egusphere-2026-2540
Preprint. Discussion started: 13 May 2026

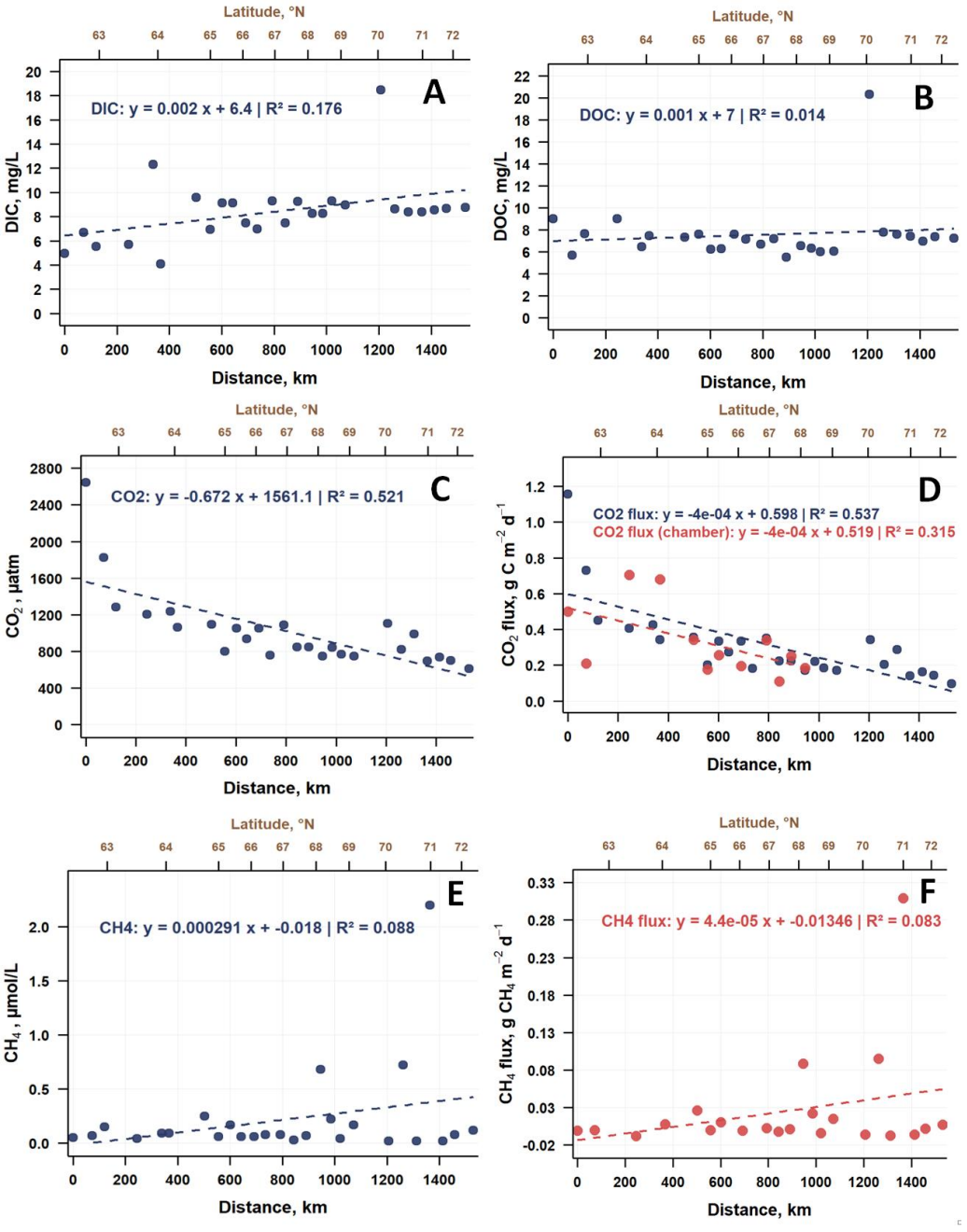

Fig. 2. Spatial variations of DIC (**A**), DOC (**B**), pCO_2 (**C**), FCO_2 (**D**), CH_4 concentration (**E**) and FCH_4 (**F**) in the main stem of the Low Lena River, from Yakutsk to Kyusur. The dots represent discrete sampling points and dashed line is a linear regression with equation parameters given on each panel.

https://doi.org/10.5194/egusphere-2026-2540
Preprint. Discussion started: 13 May 2026

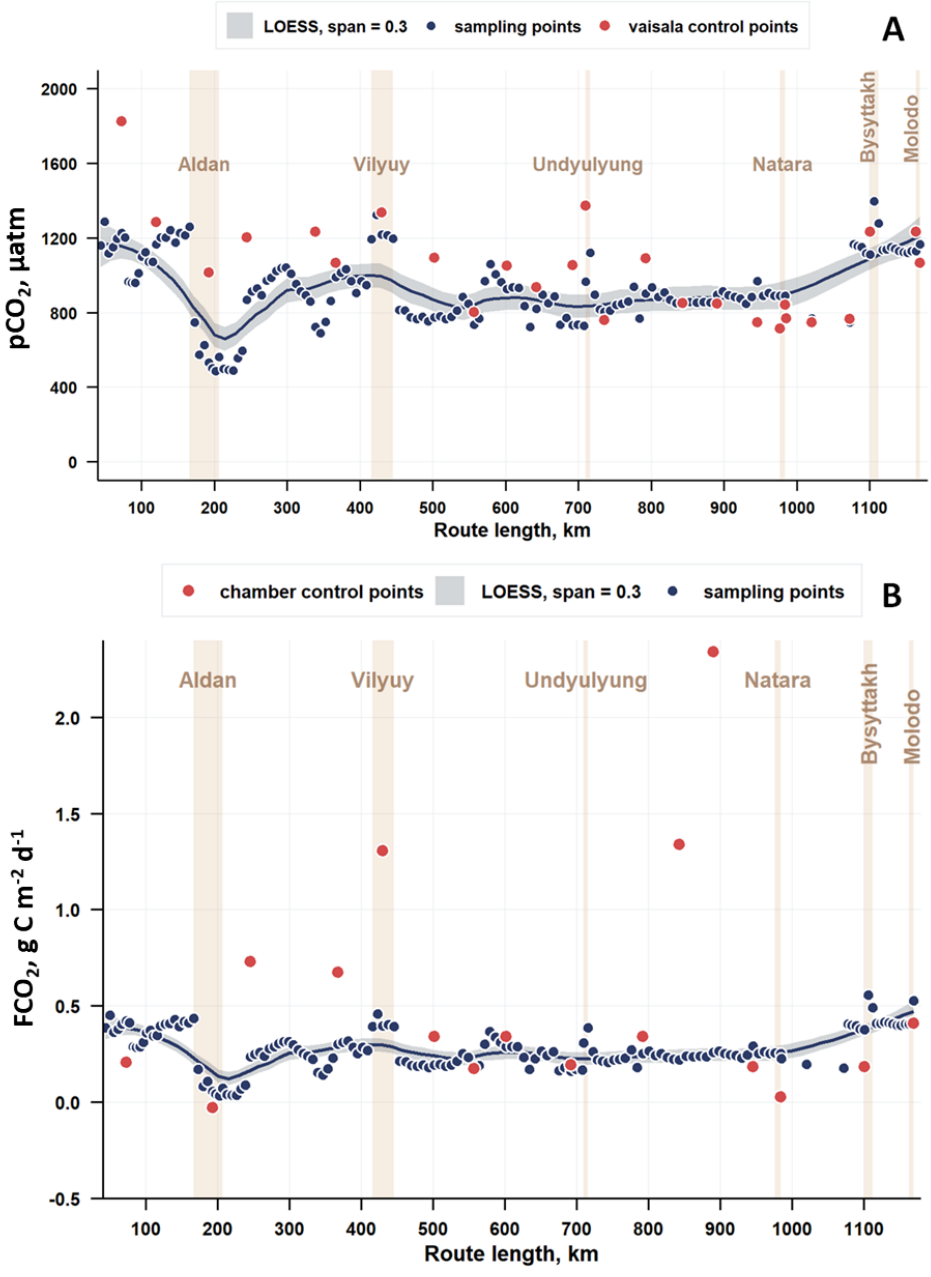

Fig. 3. Spatial variation of pCO_2 (**A**) and diffusive CO_2 flux (FCO_2) (**B**) along the Low Lena River main stem during the south–north transect. Blue symbols represent continuous in situ measurements, whereas red symbols denote control measurements obtained using an independent system (Vaisala probe for pCO_2 in **A**; floating chambers for FCO_2 in **B**). Shaded vertical bands indicate the locations of major tributaries (Aldan, Vilyui, Undyulyung, Natara, Bysyttakh, Molodo). Solid lines represent LOESS (locally estimated scatterplot smoothing) fits: span = 0.3 for continuous measurements and span = 0.8 for control datasets due to their lower number of observations (n = 24).

https://doi.org/10.5194/egusphere-2026-2540
Preprint. Discussion started: 13 May 2026

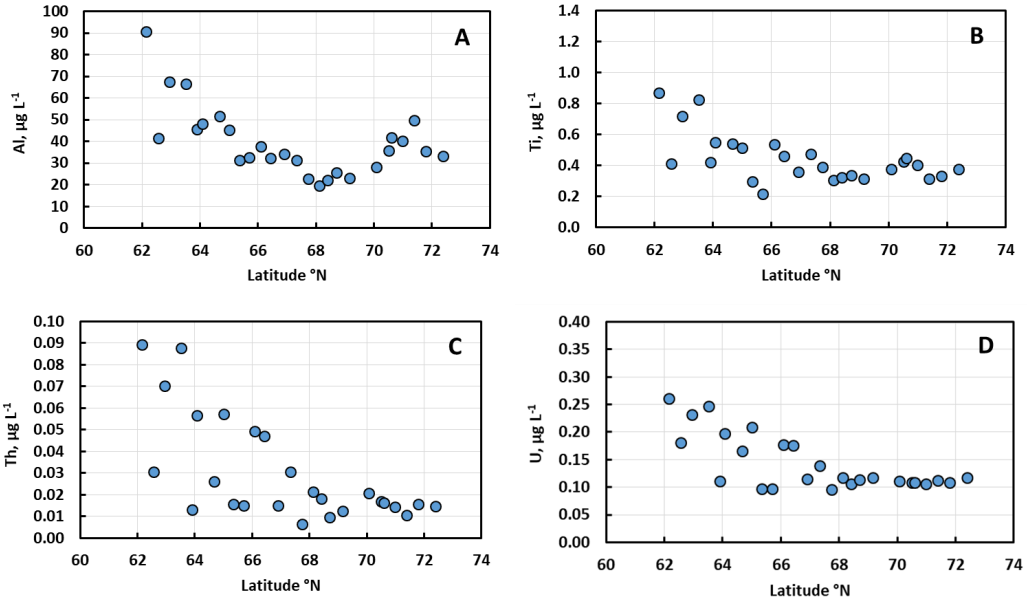

Fig. 4. Examples of low-soluble, essentially colloidal elements whose concentration in the Lena River main stem decreased northward, from Yakutsk to Kyusur: **A**, Al; **B**, Ti; **C**, Th and **D**, U.

https://doi.org/10.5194/egusphere-2026-2540
Preprint. Discussion started: 13 May 2026

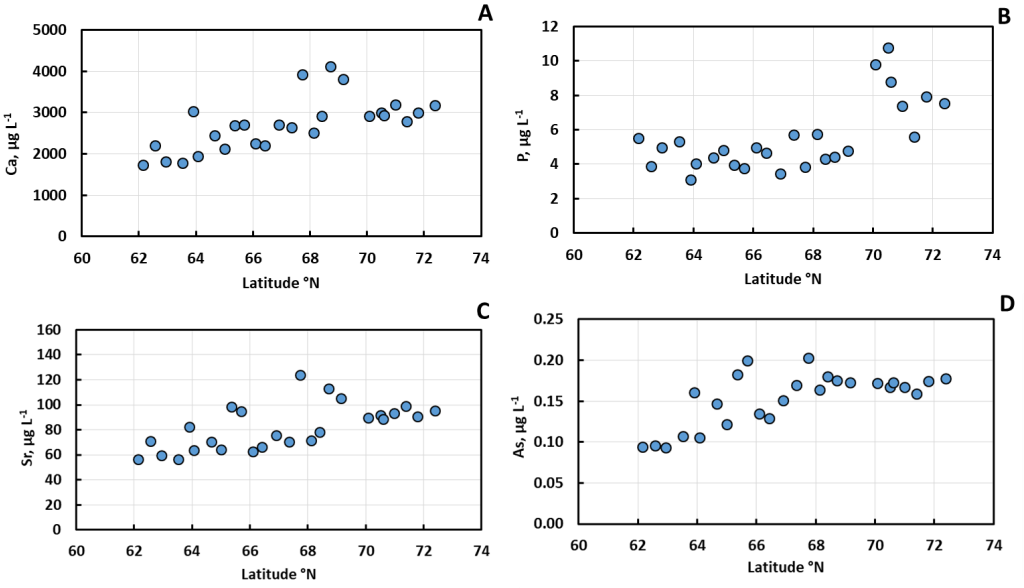

Fig. 5. Examples of labile, low colloidal elements whose concentration in the Lena River main stem increase northward, from Yakutsk to Kyusur: **A**, Ca; **B**, P; **C**, Sr and **D**, As.

https://doi.org/10.5194/egusphere-2026-2540
Preprint. Discussion started: 13 May 2026

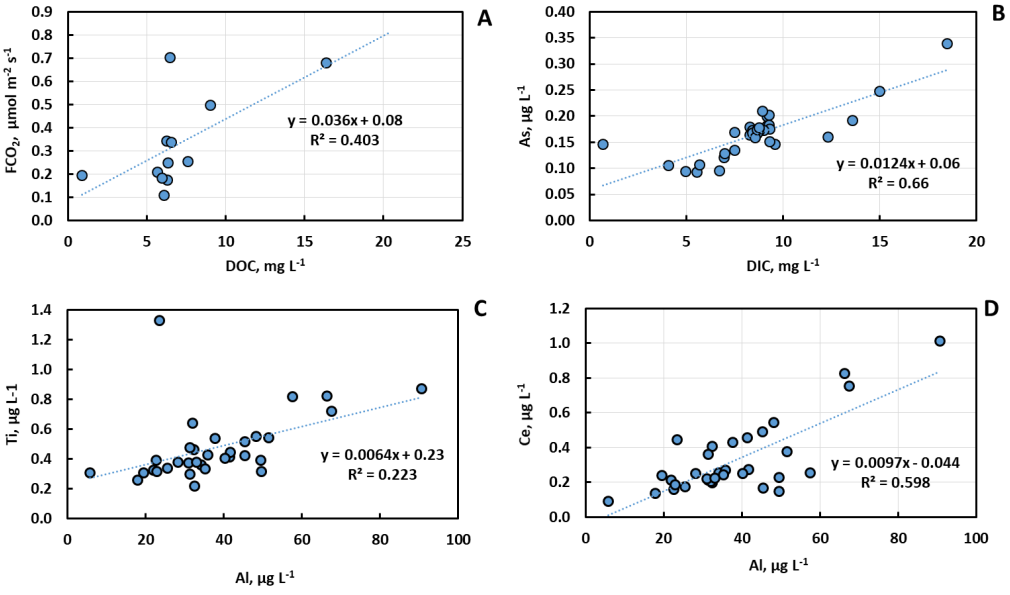

Fig. 6. Linear relationships in the Lena River and tributaries, between concentrations of DOC and FCO_2 (**A**), DIC and As (**B**) and dissolved Al as indicator of Ti (**C**) and Ce (**D**) mobility.

https://doi.org/10.5194/egusphere-2026-2540
Preprint. Discussion started: 13 May 2026

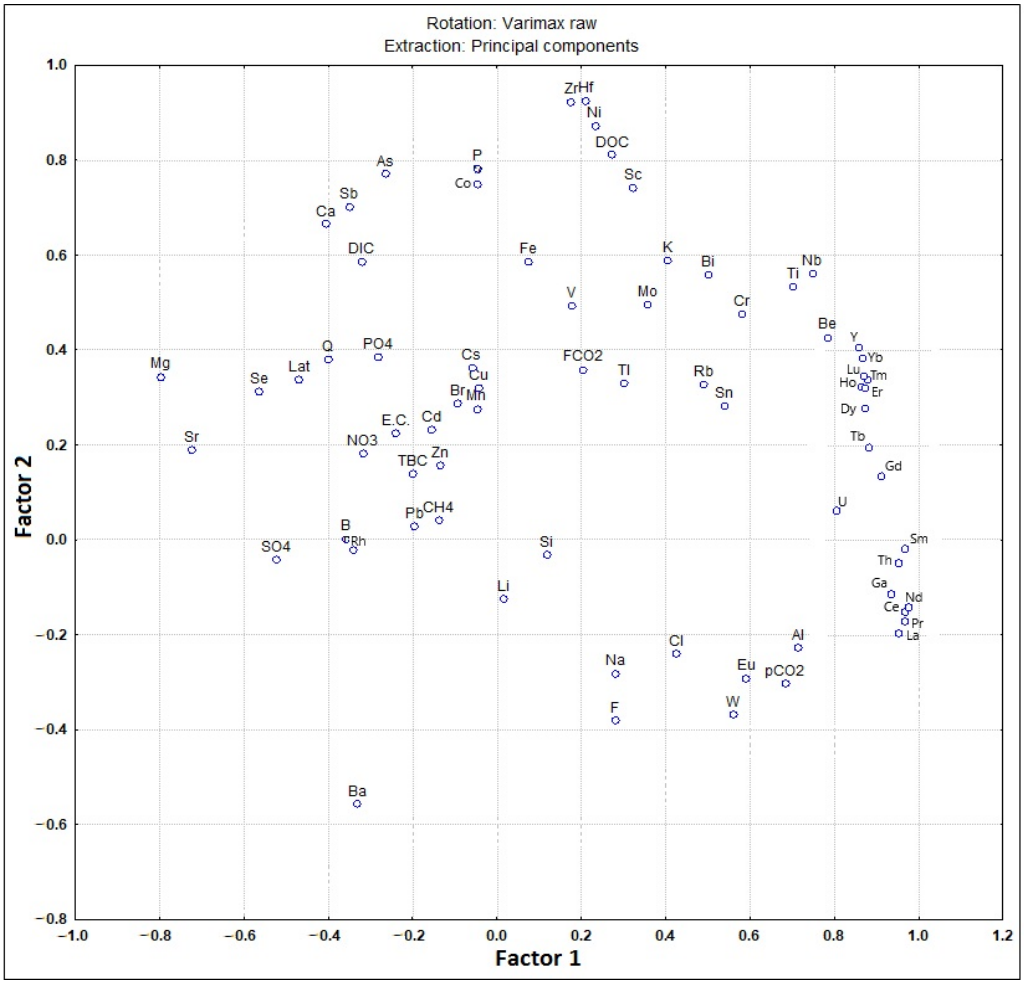

Fig. 7. Principal component analysis (PCA) of hydrochemical parameters measured in the Lena River main stem. The plot shows the loadings of dissolved gases, nutrients, major ions, and trace elements on the first two principal components (Factor 1 and Factor 2) after Varimax rotation. Factor 1 primarily separates lithogenic and conservative solutes (e.g., Al, rare earth elements, Cl, Na, and pCO_2) from elements more strongly associated with organic and colloidal phases, whereas Factor 2 reflects variability linked to dissolved organic carbon (DOC), redox-sensitive elements, and carbonate system parameters (e.g., DIC and FCO_2). Clustering of rare earth elements and several lithogenic tracers on the positive side of Factor 1 indicates a coherent mineral-derived signal, while DOC and associated metals plot toward the upper part of the diagram, suggesting an influence of organic complexation and colloidal transport.

https://doi.org/10.5194/egusphere-2026-2540
Preprint. Discussion started: 13 May 2026

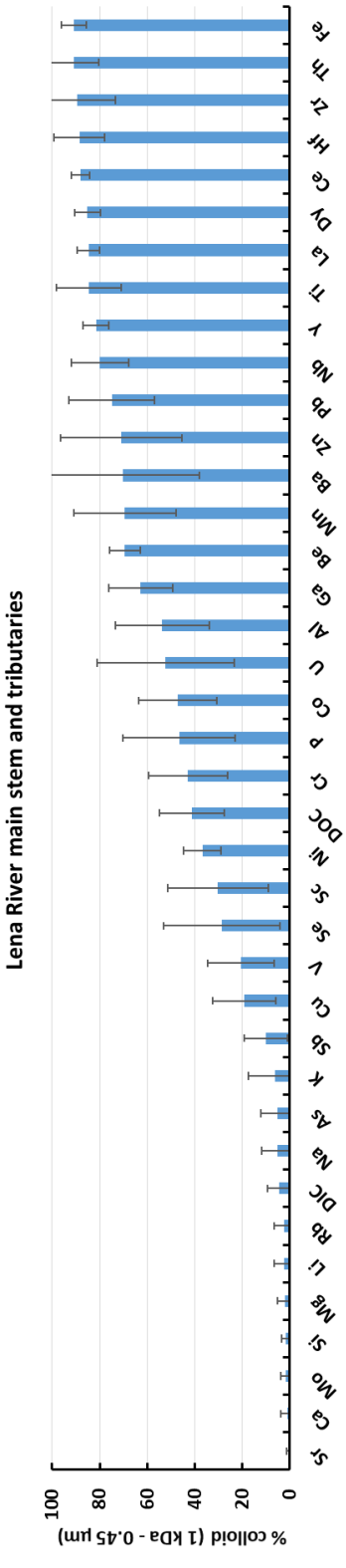

Fig. 8. Average (± s.d., n = 12) proportion of colloidal forms of major and trace elements in the Lena River and tributaries measured by dialysis procedure.